Ecol Res (2015) 30: 247–266
DOI 10.1007/s11284-014-1222-6

SPECIAL FEATURE

Long-term and interdisciplinary research on forest ecosystem functions: Challenges at Takayama site since 1993

**Hibiki M. Noda · Hiroyuki Muraoka
Kenlo Nishida Nasahara · Nobuko Saigusa
Shohei Murayama · Hiroshi Koizumi**

Phenology of leaf morphological, photosynthetic, and nitrogen use characteristics of canopy trees in a cool-temperate deciduous broadleaf forest at Takayama, central Japan

Received: 17 June 2014 / Accepted: 17 November 2014 / Published online: 2 December 2014

Abstract We studied interannual variations in single-leaf phenology, i.e., temporal changes in leaf ecophysiological parameters that are responsible for forest canopy function, in a cool-temperate deciduous broadleaf forest at Takayama, central Japan. We conducted long-term in situ research from 2003 to 2010 (excluding 2008). We measured leaf mass per unit area (LMA), leaf chlorophyll and nitrogen contents, and leaf photosynthetic and respiratory characteristics [dark respiration, light-saturated photosynthetic rate (A_{max}), maximum carboxylation rate (V_{cmax}), and electron transport rate (J_{max})] of leaves of mature canopy trees of *Betula ermanii* Cham. and *Quercus crispula* Blume, from leaf expansion to senescence. All leaf characteristics changed markedly from leaf expansion (late May) through senescence (mid–late October). The photosynthetic capacity of *B. ermanii* leaves rapidly increased during leaf expansion and decreased during senescence, while that of *Q. crispula* leaves changed gradually. The relationships among LMA, photosynthetic capacity, and nitrogen content changed throughout the season. The timings (calendar dates) of leaf expansion, maturity, and senescence differed among the 7 years, indicating that interannual variations in micrometeorological conditions strongly affected leaf phenological events. We examined the seasonal changes as a function of the date or cumulative air temperatures. From leaf expansion to maturity, the increases in chlorophyll content, A_{max}, V_{cmax}, J_{max}, and LMA were explained well by the growing-degree days, and their decreases in autumn were explained well by chilling-degree days. Our findings will be useful for predicting the effects of current variations in climatic conditions and future climate change on forest canopy structure and function.

Keywords Carbon cycle · Forest canopy · Phenology model · Photosynthesis · Respiration

H. M. Noda (✉) · N. Saigusa
Center for Global Environmental Research, National Institute for Environmental Studies, 16-2 Onogawa, Tsukuba, Ibaraki 305-8506, Japan
E-mail: noda.hibiki@nies.go.jp
Tel.: +81(29)850-2981
Fax: +81(29)850-2219

H. Muraoka
Institute for Basin Ecosystem Studies, Gifu University, 1-1 Yanagido, Gifu 501-1193, Japan

K. N. Nasahara
Faculty of Life and Environment Sciences, University of Tsukuba, 1-1-1 Tennohdai, Tsukuba, Ibaraki 305-8572, Japan

S. Murayama
Research Institute for Environmental Management Technology, National Institute of Advanced Industrial Science and Technology (AIST), AIST Tsukuba West, 16-1 Onogawa, Tsukuba 305-8569, Japan

H. Koizumi
Department of Biology, Faculty of Education, Waseda University, 2-2 Wakamatsucho, Shinjuku, Tokyo 162-8480, Japan

Introduction

Photosynthetic carbon gain and biomass growth in forest ecosystems are key factors in the carbon cycle of terrestrial ecosystems, and will become increasingly important with the predicted changes in the global climate (Canadell et al. 2000; Canadell and Raupach 2008; Ito 2008; Beer et al. 2010; Reichstein et al. 2013). In the past decade, many studies have reported on the carbon budget of the world's terrestrial ecosystems and described the associated ecological and micrometeorological processes. The methods used in such studies include surveys of ecological processes responsible for biomass growth and soil carbon sequestration (e.g., Ohtsuka et al. 2005; Fang et al. 2014), micrometeorological measurements of CO_2 flux (Yamamoto et al. 1999; Baldocchi et al. 2001; Saigusa et al. 2005; Owen et al. 2007), satellite remote sensing (Running et al. 2004; Piao et al. 2008), and simulation models (Bonan 1996; Ito and

Oikawa 2002; Piao et al. 2012). Integrated analyses combining the findings from these studies have revealed the spatial and temporal dynamics of carbon cycles and budgets (Canadell et al. 2000; Sasai et al. 2005; Piao et al. 2008; Ohtsuka et al. 2009). To date, however, researchers have not been able to estimate accurately the current status of these budgets, nor have they predicted their future changes from an ecophysiological viewpoint. Such estimates and predictions would provide an improved mechanistic understanding of the responses of plants and ecosystems to environmental changes (Tenhunen and Kabat 1999; Muraoka and Koizumi 2009).

The dynamics of forest-canopy photosynthesis can be predicted from the leaf-level photosynthetic responses to changes in micrometeorological conditions such as photosynthetic photon flux density (PPFD), air temperature, and CO_2 concentration (e.g., Farquhar et al. 1980; Baldocchi and Meyers 1998; Bernacchi et al. 2013), which fluctuate over short time scales (e.g., daily). In addition to short-term changes, the seasonal changes (i.e., phenology) in leaf/canopy morphology and physiology reflect the responses to environmental changes (e.g., Wilson et al. 2001; Ito et al. 2006; Muraoka et al. 2010). Recent in situ remote sensing observations of temperate forests have emphasized the functional importance of phenology in determining canopy photosynthesis (e.g., Richardson et al. 2006; Nakaji et al. 2007; Saitoh et al. 2012; Nagai et al. 2013). However, it is important to increase our understanding of leaf-level phenology with respect to photosynthesis and related components such as chlorophylls and nitrogen, because photosynthesis is the fundamental process controlling tree growth and the responses of the forest carbon cycle to environmental change. Understanding leaf-level phenology is also important from the perspective of using remote sensing to observe forests, as such observations rely on our ability to understand the mechanisms responsible for the spectral changes in the forest canopy.

The leaf phenology of deciduous trees can be characterized by the timings of leaf emergence in spring and leaf senescence and fall in autumn, which together determine the length of the growing season. These timings also strongly affect the growth and survival of individual plants (Augspurger 2008) through their effects on the carbon balance between photosynthesis and respiration at an individual plant level. Hence, they also determine the net primary production of forests (Goulden et al. 1996; Keeling et al. 1996; White et al. 1999). In addition to the length of the growing season, the phenology of single leaves (i.e., temporal changes in leaf morphological and physiological characteristics such as leaf area, leaf mass per unit area (LMA), leaf chlorophyll and nitrogen contents, and photosynthetic capacity) is responsible for the canopy carbon gain during the growing season. Our understanding of leaf ecophysiological characteristics of tall trees has progressed remarkably with technological improvements in photosynthetic measurement systems (Reich et al. 1991; Miyazawa et al. 1998; Wilson et al. 2000; Niinemets et al. 2004; Muraoka and Koizumi 2005; Hikosaka et al. 2007; Wang et al. 2008; Yasumura and Ishida 2011). These studies have demonstrated that single-leaf photosynthetic characteristics show substantial seasonal- or leaf age-dependent changes in deciduous and evergreen species. In general, the photosynthetic capacity increases from leaf expansion to leaf maturity and decreases before leaf fall. Previous studies have shown that there are temporal changes in the relationships between photosynthesis and nitrogen or LMA, and in the temperature responses of biochemical processes related to photosynthesis. Those studies have also demonstrated that the single-leaf phenology of ecophysiological parameters varies among species even within a single functional type (e.g., deciduous broadleaf trees) and even when they are growing in the same forest. The phenology of such ecophysiological characteristics is the fundamental process determining plant growth and forest canopy function. Therefore, we must expand on the current knowledge by studying the species-specific characteristics of leaf phenology and the generality of leaf phenology over multiple years. To do so, we must consider micrometeorological conditions rather than just calendar dates, since leaf biochemical and anatomical development depend so strongly on the leaf environment (e.g., Hikosaka et al. 2007).

The phenology of ecophysiological characteristics in a single leaf is driven by environmental conditions such as solar radiation, photoperiod, and air temperature (e.g., Cleland et al. 2007; Hänninen and Tanino 2011). In boreal and temperate regions, air temperature is often the main factor determining the timings of phenological events (Kramer et al. 2000; Peñuelas et al. 2009; Chmielewski and Rötzer 2002). Several studies have documented the effects of recent global warming on the timing of phenological events such as leaf emergence and leaf fall in various tree species (Walther et al. 2002) and in terrestrial vegetation at a continental scale (Myneni et al. 1997; Menzel et al. 2006; Piao et al. 2006). Therefore, a more comprehensive understanding of leaf phenological responses to changing temperatures will improve the accuracy of predictions of forest carbon gain under current and future climate change scenarios (Morin et al. 2010; Richardson et al. 2010; Chung et al. 2013). Considering the interannual variations in phenology, such studies should include long-term monitoring over multiple years.

The forest at the Takayama site in Japan is a cool-temperate deciduous broadleaf forest. Long-term multidisciplinary research at this site has quantified the micrometeorological and ecological processes governing the carbon budget of the forest, as well as the degree of interannual variation in the ecological processes of forest carbon assimilation and release (Yamamoto et al. 1999; Saigusa et al. 2005; Yamamoto and Koizumi 2005; Muraoka and Koizumi 2009; Ohtsuka et al. 2009). A model analysis suggested that interannual variations in leaf phenology and summer meteorological conditions

are responsible for variations in the forest carbon budget as a result of interannual changes in canopy photosynthesis (Muraoka et al. 2010).

In this study, we focused on the major canopy trees *Quercus crispula* Blume and *Betula ermanii* Cham. at the Takayama site. The aims of this study were as follows: (1) to clarify the phenological patterns of leaf photosynthetic capacity and related physiological characteristics, and (2) to identify patterns in these characteristics of deciduous broadleaf trees by examining the phenological dependency on temperature. The results of this ecophysiological study will improve our understanding of ecosystem-scale responses to environmental changes, and help to improve the accuracy of predictions about future responses to climate change.

Materials and methods

Study site and plant species

Field measurements were conducted in a cool-temperate deciduous broadleaf forest (36°08′N, 137°25′E, 1420 m a.s.l.) on the northwestern slope of Mt. Norikura, in central Japan. The Takayama study site belongs to the AsiaFlux network (http://asiaflux.net/) and the JaLTER network (http://www.jalter.org/). Researchers have investigated the carbon cycle and the CO_2 exchanges between this forest and the atmosphere using micrometeorological measurements (Yamamoto et al. 1999; Saigusa et al. 2005; Murayama et al. 2010), ecological process research (Mo et al. 2005; Muraoka and Koizumi 2005; Ohtsuka et al. 2007, 2009; Nasahara et al. 2008), process-based modeling (Ito et al. 2006; Muraoka et al. 2010), and remote sensing (Muraoka and Koizumi 2009; Nagai et al. 2010). Table 1 shows air temperature and precipitation during the growing season (April to October) at the forest. The site is covered by snow from December until April, and its peak depth ranges from 100 to 180 cm. The forest canopy is dominated by *Q. crispula*, *Betula platyphylla* Sukatchev var. *japonica* Hara, and *B. ermanii*. The subcanopy and shrub layers are dominated by *Acer rufinerve* Sieb. et Zucc., *Acer distylum* Sieb. et Zucc., *Hydrangea paniculata* Sieb., and *Viburnum furcatum* Blume ex Maxim. The understory is dominated by an evergreen dwarf bamboo, *Sasa senanensis* (Fr. et Sav.) Rehder, with a height of 1.0–1.5 m. The height of the dominant forest canopy ranges from 13 to 20 m. All of the deciduous tree species flush their leaves after snowmelt in mid-May and lose their leaves by late October or early November.

In this study, we focused on the sun leaves of *B. ermanii*, which has a thin crown, and the sun and shade leaves of *Q. crispula*, which has a multi-layered crown. The sun leaves of *B. ermanii* and *Q. crispula* were obtained from the top of the crown or from a south-facing branch. The shade leaves of *Q. crispula* were obtained from the middle of the crown (ca. 7 m above the ground). In 2006, the monthly average of relative PPFD (measured using IKS-27 PPFD sensors; Koito, Yokohama, Japan), which is the ratio of daily PPFD measured at the height of the shade leaves to the open sky PPFD, was 32.9 % in May, 6.7 % in June, 3.5 % in July, 3.3 % in August, and 4.3 % in September.

Measurements of leaf ecophysiological traits

We conducted our measurements of canopy leaves during the growing season, from budburst in mid-May to senescence at the end of October. Measurements were conducted from 2003 to 2010 (except for 2008) for *B. ermanii* and *Q. crispula* sun leaves and from 2003 to 2006 and in 2010 for *Q. crispula* shade leaves. *Quercus crispula* has a single leaf flush, which occurs within a single short period in the early growing season, whereas *B. ermanii* shows indeterminate leaf production and can produce several consecutive leaf flushes (Koike 1988). In this forest, *B. ermanii* produces two leaf flushes, the first in mid-May and the second in early June. Typically, more than half of the leaves from the second flush are lost to herbivores (data not shown); therefore, we focused on the leaves from the first flush. We measured leaf CO_2 gas-exchange traits, chlorophyll content, nitrogen content, and LMA for the same sample leaves on each measurement day. The measurements were conducted once every 2–4 weeks. However, we were unable to obtain some measurements because of the rapid change in

Table 1 Climatic conditions at the Takayama study site from 2003 to 2010

	Monthly mean air temperature (°C)							Mean air temperature from April to October (°C)	Annual mean air temperature (°C)	Precipitation from April to October (mm)
	Apr.	May	Jun.	Jul.	Aug.	Sep.	Oct.			
2003	5.8	10.4	14.2	15.1	18.1	15.0	7.9	12.4	6.3	1407
2004	5.9	11.4	15.2	19.0	18.4	15.9	9.2	13.6	7.3	1742
2005	6.0	9.1	15.3	17.6	18.2	15.9	9.4	13.1	6.0	1106
2006	3.2	10.2	14.9	17.3	19.6	14.3	10.1	12.8	6.7	1401
2007	3.2	9.4	13.6	16.5	19.2	16.6	9.0	12.5	6.7	1266
2008	5.3	10.5	13.7	18.7	18.5	14.9	9.5	13.0	6.6	1197
2009	5.5	11.1	14.2	17.2	17.8	13.7	8.9	12.6	6.8	1448
2010	3.4	9.4	15.1	18.7	20.2	15.8	9.9	13.2	7.1	1811

leaf size during the expansion period or unsuitable weather conditions at the study site.

Leaf photosynthetic CO_2 gas exchange measurements were conducted from a canopy-access tower (18-m height) using a portable photosynthesis measuring system (LI-6400, Li-Cor, Inc., Lincoln, NE, USA). We measured three to five representative leaves of each species and their light environments in the morning (from 0800 to 1200 h) to avoid the influences of midday stomatal closure and photoinhibition. The dark respiration rate (R) and the relationship between the net photosynthetic rate (A) and leaf intercellular CO_2 partial pressure (C_i) were determined to obtain the leaf photosynthetic characteristics and to quantify net photosynthesis. The relationships between A and C_i were obtained under saturating PPFD (provided by the red–blue LED of the LI-6400) and a leaf-to-air vapor-pressure deficit of < 1.2 kPa. The temperature conditions during measurements were adjusted using the fan and Peltier device of the LI-6400 to match the ambient conditions in each season (9–19 °C in May and October; 14–24 °C in June, July, and September; and 21–27 °C in August). For the sun leaves of both species, at least one entire curve for the relationship between A and C_i was obtained during each field measurement period by adjusting the concentration of CO_2 entering the leaf chamber (C_a) from 0 to 1500 μmol CO_2 mol^{-1} air. Since the measurement of A/C_i curves was time consuming, we measured the photosynthetic rates only at ambient and high CO_2 concentrations and dark respiration to increase the number of samples.

We used the one-point method (Wilson et al. 2000; Kosugi et al. 2003; Wang et al. 2008) to calculate the photosynthetic parameters. The maximum carboxylation rate (V_{cmax}) was calculated using data from the range in which ribulose bisphosphate is saturated ($C_a < 370$ μmol mol^{-1}). The photosynthetic rate (A_c) was calculated as a function of C_i and V_{cmax} using the following equation:

$$A_c = \frac{V_{cmax}(C_i - \Gamma^*)}{C_i + K_c(1 + O/K_o)} - R_d, \quad (1)$$

where K_c and K_o are the Michaelis–Menten constants of Rubisco for CO_2 and O_2, respectively; O is the O_2 concentration; Γ^* is the CO_2 compensation point in the absence of photorespiration; and R_d is the photorespiration rate, which is assumed to be 40 % of R. We used the generic temperature responses of Γ^*, K_o, and K_c from Bernacchi et al. (2001). The potential rate of electron transport (J_{max}) was calculated from the photosynthetic rate (A_j) at which ribulose bisphosphate regeneration is the limiting factor ($C_a > 1000$ μmol mol^{-1}), as follows:

$$A_j = \frac{J(C_i - \Gamma^*)}{4C_i + 8\Gamma^*} - R_d, \quad (2)$$

where J is the actual rate of electron transport. J is related to the incident PPFD (Q), and J_{max} was estimated by solving the following equation:

$$\theta J^2 - (\alpha Q + J_{max})J + \alpha Q J_{max} = 0, \quad (3)$$

where θ is the curvature of the light-response curve and α is the quantum yield of electron transport. The values of α and θ were taken to be 0.3 mol electrons mol^{-1} photon and 0.90, respectively, according to Medlyn et al. (2002). The R, V_{cmax}, and J_{max} values were standardized to the reference leaf temperature of 20 °C (R_{20}, V_{cmax20}, and J_{max20}) using the temperature-dependence equations of Harley and Baldocchi (1995).

After measuring photosynthetic CO_2 gas exchange, we collected the leaves in plastic bags and transported them to the laboratory (approx. 10 min). Leaf discs (1-cm diameter) were punched out in the laboratory and kept at −80 °C until use. Chlorophylls a and b were extracted from the leaf discs with N,N′-dimethylformamide and their concentrations were calculated from absorbance values determined with a spectrophotometer (UV-1200, Shimadzu, Kyoto, Japan) following the method of Porra et al. (1989). The residual parts of the leaves were scanned with a digital scanner and the area was estimated using image-analysis software "LIA for Win32" (http://www.agr.nagoya-u.ac.jp/~shinkan/LIA32/index-e.html). Then, the leaves were dried at 70 °C for 72 h to measure dry weight. We calculated LMA (g m^{-2}) as the ratio of leaf dry weight to leaf area. The dried leaves were ground into a powder and analyzed with an NC-analyzer (Sumigraph NC-22, Sumika Chemical Analysis Service, Ltd., Tokyo, Japan, or Flash EA 1112, Thermo Electron, Waltham, MA, USA).

Some of the leaf photosynthetic and respiratory data from 2003 have been reported previously by Muraoka and Koizumi (2005), and some of the photosynthetic data from 2003 to 2009 have been used in a modeling analysis of forest canopy photosynthesis (Muraoka et al. 2010, 2013). However, the present study is the first to analyze and report the original leaf characteristics data for the entire study period.

Estimation of leaf nitrogen allocation

Using the abovementioned data, we examined the allocation of leaf nitrogen to the photosynthetic apparatus by applying the model proposed by Niinemets and Tenhunen (1997). The photosynthetic apparatus was divided into three categories: (1) Rubisco, (2) the bioenergetics pool, and (3) the light harvesting components. In the present study, we calculated the nitrogen allocation to these three components to estimate the total nitrogen in the photosynthetic apparatus, which we used in our phenology analysis. Rubisco nitrogen (N_r) was calculated as follows:

$$N_r \text{ per unit leaf area} = \frac{V_{cmax}}{6.25V_{cr}}, \quad (4)$$

where 6.25 is the ratio of the weight of Rubisco to the weight of nitrogen in Rubisco and V_{cr} is the specific

activity of Rubisco (mmol CO_2 g^{-1} Rubisco s^{-1}). Since V_{cr} is assumed to be a function of temperature, N_r per unit leaf area was estimated using the V_{cmax} and V_{cr} values at the leaf temperature during the gas exchange measurement. V_{cr} at that temperature was calculated according to Niinemets and Tenhunen (1997). The amount of nitrogen in the bioenergetics pool (N_b) was calculated as follows:

$$N_b \text{ per unit leaf area} = \frac{J_{max}}{8.06 J_{mc}}, \quad (5)$$

where 8.06 is the amount of nitrogen in the bioenergetics pool per unit cytochrome f (mmol cyt f (g N in bioenergetics)$^{-1}$) and J_{mc} is the photosynthetic electron transport per unit cytochrome f (mmol electrons (mmol cyt f)$^{-1}$ s^{-1}). Because J_{mc} is also a function of temperature, we used J_{max} and J_{mc} at the leaf temperature during the photosynthetic measurements to calculate N_b. J_{mc} at that temperature was also calculated by the equation of Niinemets and Tenhunen (1997). The nitrogen cost for light harvesting (N_h) depends on the chlorophyll content associated with photosystems I (PSI) and II (PSII), and with the light-harvesting chlorophyll protein complex of PSII (LHCII). Thus, N_h per unit leaf area was calculated as follows:

$$N_h \text{ per unit leaf area} = C_c\left[0.46 P_{C(PSI)} + 1.17 P_{C(PSII)} + 0.36 P_{C(LHCII)}\right], \quad (6)$$

where C_c is the leaf chlorophyll content (mmol m^{-2}); $P_{C(PSI)}$, $P_{C(PSII)}$, and $P_{C(LHCII)}$ are the fractions of chlorophyll associated with PSI, PSII, and LHCII, respectively; and 0.46, 1.17, and 0.36 are the weights of nitrogen per weight of chlorophyll bound to PSI, PSII, and LHCII, respectively (Hikosaka and Terashima 1995). PSI content (mmol m^{-2}) was assumed to be $1.7 \times C_c$ (Niinemets and Tenhunen 1997), and $P_{C(PSI)}$ was calculated as follows: 1.7×0.184; where 0.184 is the amount of chlorophyll (mmol) bound to one PSI complex (Hikosaka and Terashima 1995). Because PSII content ($PSII_c$) per C_c is strongly correlated with cytochrome f content per C_c, PSII content was estimated from the C_c and cytochrome f content, which was obtained as J_{max}/J_{mc} according to Niinemets and Tenhunen (1997). $P_{C(PSII)}$ was calculated as the product of $PSII_c$ and the amount of chlorophyll bound to one PSII complex (0.06 mmol; Hikosaka and Terashima 1995). The amount of chlorophyll associated with LHCII was assumed to be the difference between C_c and the chlorophyll associated with PSI and PSII. Thus, $P_{C(LHII)}$ was calculated as follows: $1-P_{C(PSI)}-P_{C(PSII)}$. The amount of nitrogen in the photosynthetic apparatus (N_{ph}) equaled the sum of N_r, N_b, and N_h.

Modeling phenology of leaf morphological and physiological traits

We examined the seasonal changes in leaf characteristics as a function of air temperature. To model aspects of leaf development (chlorophyll content, A_{max}, V_{cmax20}, J_{max20}, and LMA) against air temperature during the growing season (from spring to the end of summer) we calculated the growing-degree days (GDD) index using the following equation:

$$GDD_k(t) = \sum_{i=1}^{t} \max(T_i - k, 0), \quad (7)$$

where t is time (day of year, DOY), T_i is daily mean air temperature on DOY i, and k is a threshold temperature. To test the threshold temperature for leaf development, GDD was calculated with three temperatures; 0, 2 and 5 °C. The changes in chlorophyll content, A_{max}, V_{cmax20}, and J_{max20} during the senescence period from late summer to autumn were examined by calculating the chilling-degree days (CDD) index. The CDD index from DOY 213 (31 July or 1 August) to DOY 365 (30 or 31 December) was calculated using the following equation:

$$CDD_k(t) = \sum_{i=213}^{t} \min(T_i - k, 0). \quad (8)$$

The values of k for CDD were set to 15, 18, and 20 °C. The changes in GDD_0 and CDD_{18} as a function of DOY are shown in Fig. 1.

In previous studies, canopy phenology was characterized as a simple sigmoid-shaped logistic function based on DOY (Zhang et al. 2003; Richardson et al. 2007; Ide and Oguma 2010). In the present study, we examined a logistic function based on DOY and GDD or CDD to characterize the seasonal changes in ecophysiological parameters:

$$f(x) = a + \frac{b}{1 + \exp(c - dx)}. \quad (9)$$

The data during the development period (DOY $\leq$ 240) were fitted to the models with x = DOY, GDD_0, GDD_2, and GDD_5. For the data during the senescence period (DOY $>$ 240), we tested models based on DOY, CDD_{15}, CDD_{18} and CDD_{20}. To apply this function to the senescence period, in which the calendar date is the independent variable, we used the opposite values of DOY [i.e., DOY $\times$ (−1)] since all of the CDD values are negative by definition. The parameters a and b control the lower limit (a) and the upper limit ($a + b$) of the function. The c parameter causes parallel shifts in the response to the driving variable x (here, either DOY, GDD, the opposite of DOY, or CDD), and changes in the parameter d affect the overall steepness of the re-

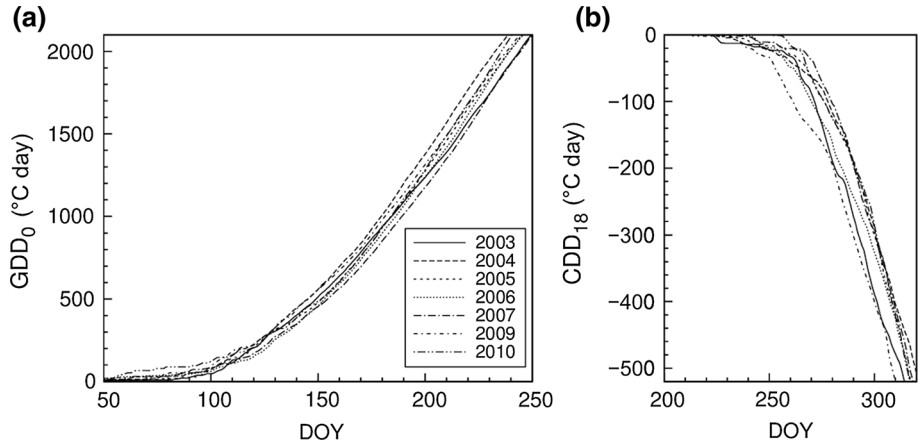

Fig. 1 **a** Growing-degree days above 0 °C (GDD_0) and **b** chilling-degree days below 18 °C (CDD_{18}) as a function of day of year (DOY) from 2003 to 2010

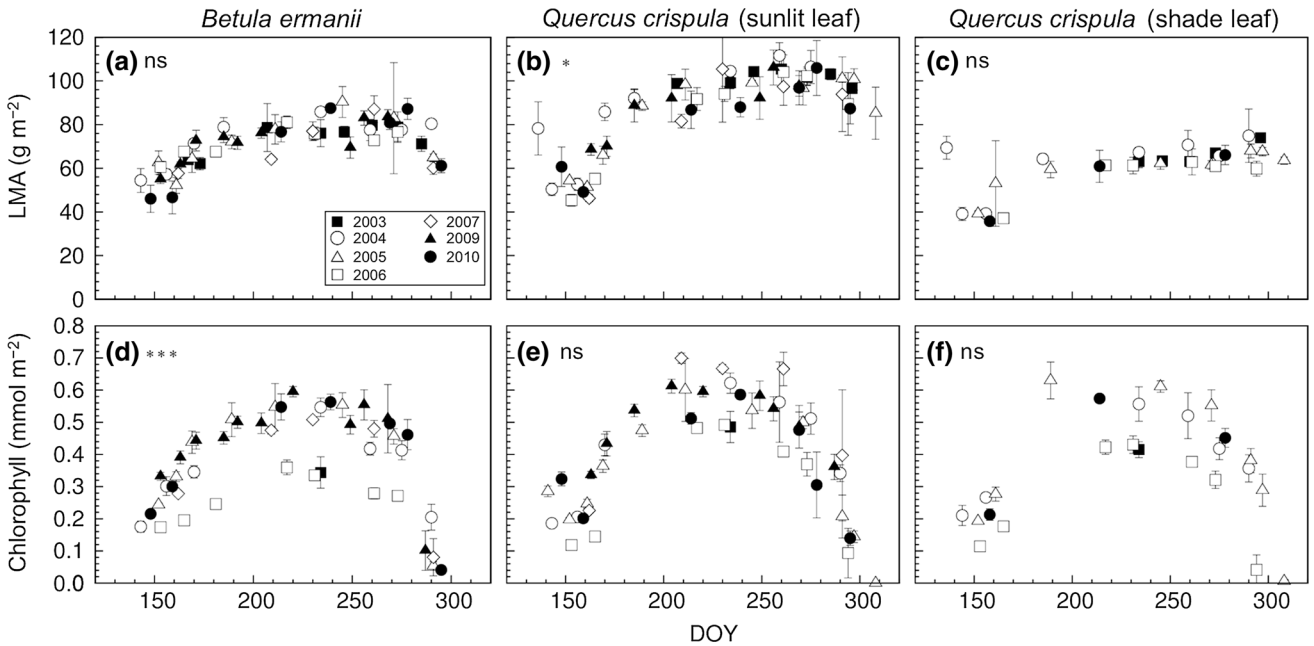

Fig. 2 Seasonal changes in **a**, **b**, **c** leaf mass per unit area (LMA) and **d**, **e**, **f** chlorophyll content. *Asterisks* or "*ns*" indicate significance of interannual variations (ns: *p > 0.05; **p < 0.05; ***p < 0.01; **** < 0.001; ANOVA). Values are mean ± SD (n = 3–5 leaves)

sponse to the driving variable. The c parameter is positive for the leaf development model and negative for the leaf senescence model. In the leaf senescence models for chlorophyll content, A_{max}, and V_{cmax}, the values for parameter b were the same as those used in the corresponding leaf development models.

Statistical analysis

To examine the interannual variations in LMA, chlorophyll content, R_{20}, A_{max}, V_{cmax20} and J_{max20}, one-way ANOVA was conducted using the free statistical software GNU R (R Core Team 2014, http://www.R-project.org/).

Results

Seasonal and interannual variations in leaf characteristics

Figure 2 shows the seasonal and interannual variations in LMA and chlorophyll contents of *B. ermanii* and *Q. crispula* leaves, and Table 2 summarizes the peak values of each parameter and its DOY. In all leaves, LMA increased remarkably from leaf emergence until midsummer (late July; ca. DOY 200), increased more slowly until late September, and then declined until leaf fall in October (Fig. 2a, b, c; Table 2). The high LMA values

Table 2 Peak values of LMA, chlorophyll content, A_{max},V_{cmax20}, and J_{max20} for two tree species from 2003 to 2010. Values shown are mean ± SD (n = 3–5 leaves) and day of year (DOY) of the peak value

Year	Peak LMA (g m^{-2})	DOY of peak LMA	Peak Chl. (mmol m^{-2})	DOY of peak Chl.	Peak A_{max} (μmol m^{-2} s^{-1})	DOY of peak A_{max}	Peak V_{cmax20} (μmol m^{-2} s^{-1})	DOY of peak V_{cmax20}	Peak J_{max20} (μmol m^{-2} s^{-1})	DOY of peak J_{max20}
Betula ermanii										
2003	79.69 ± 1.28	260	——	——	17.73 ± 1.16	246	55.27 ± 5.34	260	128.49 ± 13.59	260
2004	85.90 ± 0.76	234	0.55 ± 0.03	234	15.17 ± 0.78	234	47.71 ± 1.45	234	104.98 ± 5.55	234
2005	90.38 ± 7.08	245	0.55 ± 0.04	245	15.87 ± 1.23	211	49.14 ± 3.91	211	110.89 ± 12.79	271
2006	81.06 ± 2.88	217	0.36 ± 0.02	217	15.63 ± 1.67	231	50.62 ± 5.56	231	106.53 ± 5.98	217
2007	87.11 ± 6.09	261	0.51 ± 0.01	230	14.73 ± 1.09	230	51.19 ± 3.57	230	97.60 ± 1.33	209
2009	83.47 ± 3.40	268	0.60 ± 0.02	220	14.22 ± 0.89	192	45.94 ± 2.45	192	109.99 ± 9.13	171
2010	87.58 ± 2.95	239	0.56 ± 0.02	239	15.78 ± 1.05	214	47.88 ± 3.68	214	107.68 ± 9.26	269
Mean		246.3		230.8		222.6		224.6		233.0
Quercus crispula (sun leaf)										
2003	105.38 ± 8.00	260	——	——	14.93 ± 0.87	246	49.84 ± 2.77	246	124.05 ± 8.59	260
2004	121.32 ± 4.46	290	0.62 ± 0.03	234	15.27 ± 1.13	234	51.28 ± 3.79	234	107.19 ± 5.19	259
2005	101.08 ± 1.63	291	0.60 ± 0.10	211	14.60 ± 0.96	211	48.68 ± 2.99	211	105.45 ± 11.79	271
2006	104.08 ± 7.90	261	0.49 ± 0.01	231	17.23 ± 0.91	231	57.95 ± 2.20	231	118.28 ± 6.44	231
2007	105.46 ± 24.30	230	0.70 ± 0.02	209	16.80 ± 1.99	230	53.07 ± 7.81	230	124.02 ± 13.32	230
2009	106.17 ± 8.02	256	0.61 ± 0.02	202	10.75 ± 1.37	256	36.80 ± 4.30	256	107.90 ± 6.23	256
2010	105.98 ± 12.60	278	0.59 ± 0.01	239	12.47 ± 1.35	214	44.07 ± 0.16	239	93.21 ± 10.63	269
Mean		266.6		221.0		231.7		235.3		253.7
Quercus crispula (shade leaf)										
2003	73.92 ± 0.57	296	——	——	7.60 ± 0.02	246	25.81 ± 1.88	173	56.40 ± 4.24	273
2004	74.92 ± 12.26	290	0.56 ± 0.05	234	9.56 ± 0.87	234	30.77 ± 2.18	234	59.47 ± 17.94	234
2005	67.94 ± 3.18	291	0.63 ± 0.06	189	10.12 ± 1.25	189	34.42 ± 3.29	189	77.04 ± 3.76	189
2006	62.91 ± 5.97	261	0.43 ± 0.03	231	8.74 ± 0.18	217	30.65 ± 9.28	231	55.72 ± 14.34	261
2010	66.01 ± 4.43	278	0.57 ± 0.01	214	7.54 ± 0.92	214	25.32 ± 3.32	214	59.84 ± 5.35	278
Mean		283.2		217.0		220.0		208.2		247.0

A_{max} light-saturated photosynthetic rate, V_{cmax20} maximum carboxylation rate at 20 °C, J_{max20} potential electron transport rate at 20 °C, LMA leaf mass per unit area

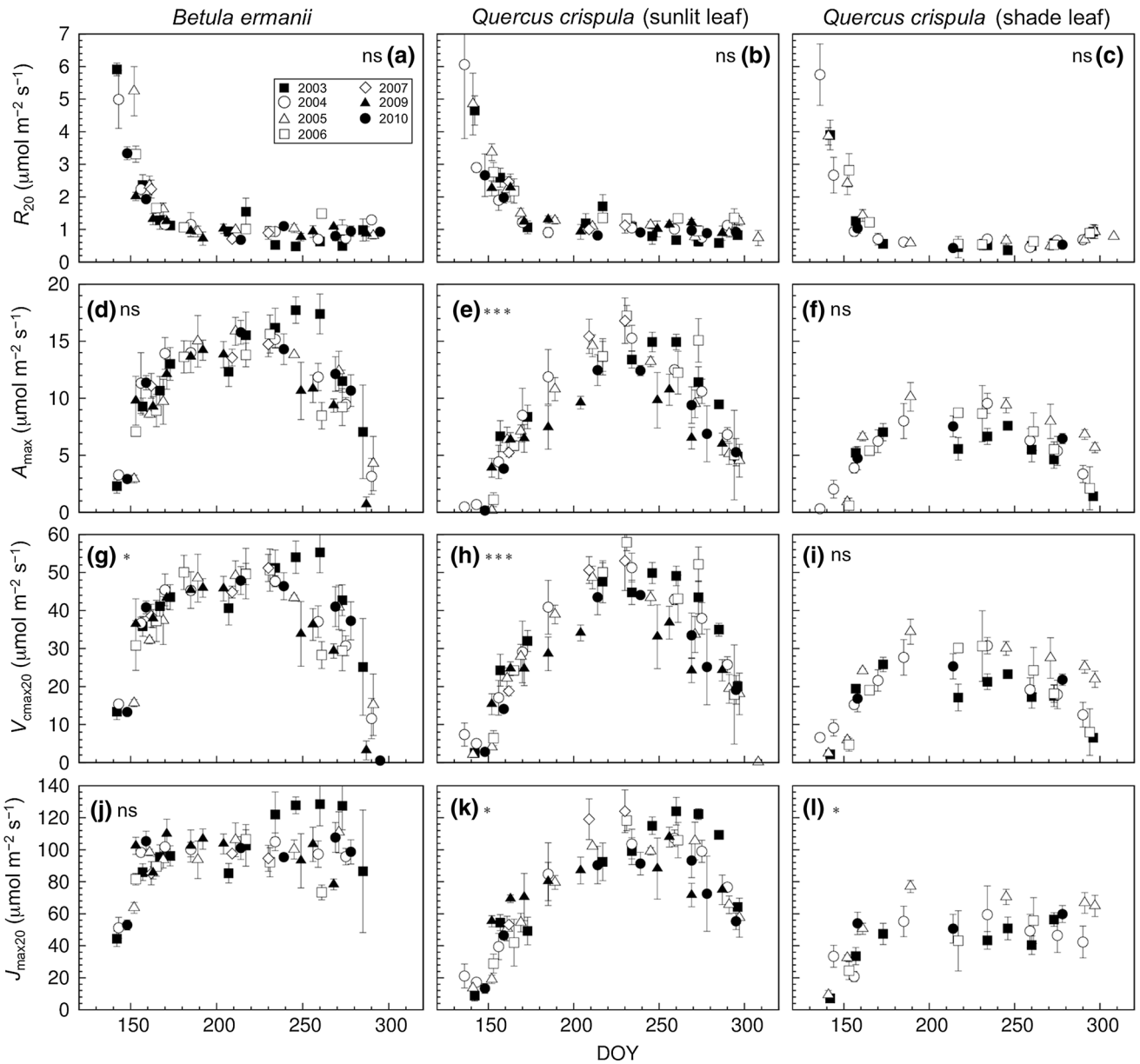

Fig. 3 Seasonal changes in **a**, **b**, **c** dark respiration rate at 20 °C (R_{20}), **d**, **e**, **f** light-saturated photosynthetic rate (A_{max}), **g**, **h**, **i** maximum carboxylation rate at 20 °C (V_{cmax20}), and **j**, **k**, **l** potential electron transport rate at 20 °C (J_{max}). *Asterisks* or "*ns*" indicate significance of interannual variations (ns: * p > 0.05; **p < 0.05; ***p < 0.01; < ****0.001; ANOVA). Values are mean ± SD (n = 3–5 leaves)

in sun and shade leaves of *Q. crispula* at the beginning of leaf expansion were because the very young leaves were folded and shrunken; thus, the measurements underestimated the actual leaf area. Throughout the growing season, the LMA of *Q. crispula* sun leaves varied among years ($p < 0.05$), while the LMA of *B. ermanii* leaves and *Q. crispula* shade leaves did not show interannual variations ($p > 0.05$; Fig. 2a, b, c). Chlorophyll content increased rapidly from leaf expansion until late July/early August (Fig. 2d, e, f; Table 2) and then decreased to almost zero in late October. Although the seasonal patterns were similar in all years, the absolute values of chlorophyll content in *B. ermanii* leaves varied among the years ($p < 0.001$); the chlorophyll content was lower in 2006 than in other years (maximum value in 2006 was 35 % lower than that in 2005).

Leaf photosynthetic and respiratory characteristics also showed remarkable seasonal changes (Fig. 3). The R_{20} was highest immediately after leaf emergence, then it decreased rapidly until mid-June (DOY 165), and then stabilized until leaf yellowing began in the autumn (Fig. 3a, b, c). There were almost parallel changes in A_{max}, V_{cmax20}, and J_{max20} throughout the growing season, but the peak in J_{max20} tended to be later than the

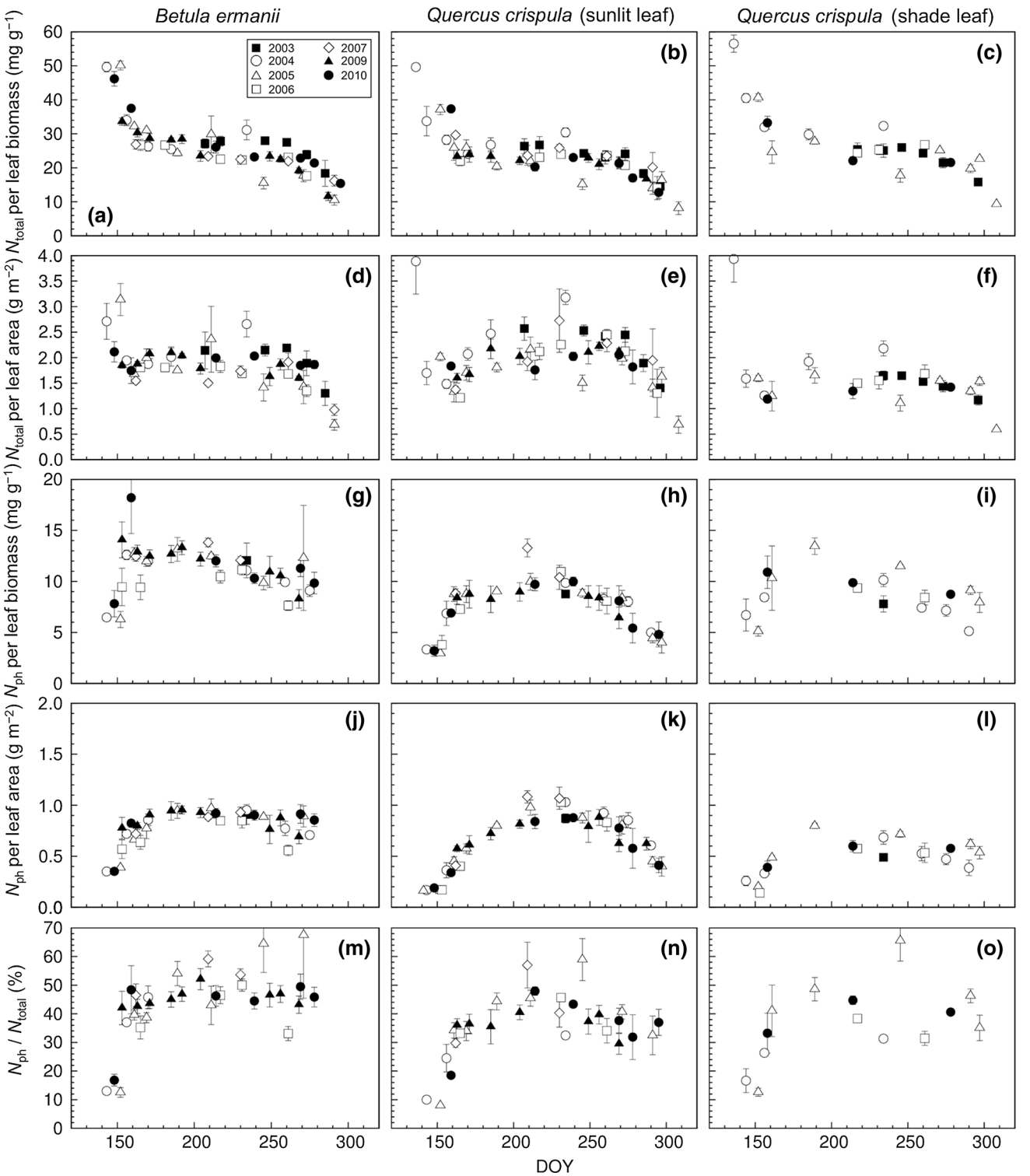

Fig. 4 Seasonal changes in (**a**, **b**, **c**) total leaf nitrogen (N_{total}) per unit leaf biomass, (**d**, **e**, **f**) N_{total} per unit leaf area, (**g**, **h**, **i**) nitrogen in photosynthetic apparatus (N_{ph}) per unit leaf area, (**j**, **k**, **l**) N_{ph} per unit leaf biomass, and (**m**, **n**, **o**) ratio of N_{ph} to N_{total}. Values are mean ± SD (n = 3–5 leaves)

peaks in A_{max} and V_{cmax20} in all leaves (Table 2). The values of A_{max}, V_{cmax20}, and J_{max20} increased from leaf emergence until late August in *Q. crispula* sun leaves, but increased rapidly until early July or mid-August in *B. ermanii* leaves (Table 2). In all leaves, A_{max} and V_{cmax20} started to decrease in late August. The J_{max20} started to decrease in the sun leaves of *Q. crispula* in late August, but we could not find a clear trend in J_{max20} in *B. ermanii*

Table 3 Coefficients of determination (r^2) for logistic models of phenological changes in ecophysiological traits during leaf development and leaf senescence periods

Development model	x	Chl.	A_{max}	V_{cmax20}	J_{max20}	LMA
Betula ermanii	DOY	0.557	0.755	0.744	0.567	0.645
	GDD_0	0.602	**0.763**	**0.753**	**0.610**	0.666
	GDD_2	**0.605**	0.752	0.733	0.591	0.668
	GDD_5	0.588	0.741	0.721	0.578	**0.673**
Quercus crispula (sun leaf)	DOY	0.778	**0.827**	**0.845**	0.802	0.637
	GDD_0	0.803	0.824	0.844	**0.806**	0.698
	GDD_2	**0.806**	0.822	0.842	0.801	**0.762**
	GDD_5	0.801	0.818	0.839	0.793	0.719
Quercus crispula (shade leaf)	DOY	0.699	0.797	0.721	0.338	0.270
	GDD_0	0.762	**0.801**	0.748	**0.499**	0.453
	GDD_2	**0.774**	0.798	**0.749**	0.488	**0.458**
	GDD_5	0.766	0.781	0.738	0.461	0.453
Senescence model						
Betula ermanii	DOY	**0.771**	0.598	0.551	–	–
	CDD_{15}	0.188	0.592	0.225	–	–
	CDD_{18}	0.762	**0.650**	**0.616**	–	–
	CDD_{20}	0.101	0.638	0.226	–	–
Quercus crispula (sun leaf)	DOY	0.594	**0.638**	**0.618**	**0.438**	–
	CDD_{15}	0.686	0.619	0.586	0.306	–
	CDD_{18}	**0.688**	0.622	0.592	0.342	–
	CDD_{20}	0.664	0.616	0.586	0.342	–
Quercus crispula (shade leaf)	DOY	0.630	0.535	0.426	–	–
	CDD_{15}	0.725	0.587	0.525	–	–
	CDD_{18}	**0.740**	**0.600**	**0.540**	–	–
	CDD_{20}	0.699	0.586	0.516	–	–

Models for leaf development period were based on day of year (DOY) and growing-degree days above 0, 2, and 5 °C (GDD_0, GDD_2, and GDD_5, respectively)
Models for leaf senescence period were based on opposite of DOY and chilling-degree days below 15, 18, and 20 °C (CDD_{15}, CDD_{18}, and CDD_{20}, respectively)
x is the driving variable for the models
Highest r^2 value is shown in bold type

sun leaves because of insufficient data (measurements of the photosynthetic rate at a high CO_2 concentration to determine J_{max} were difficult in that month because of rapid stomatal closure). The A_{max} and V_{cmax20} of *Q. crispula* leaves showed yearly variations ($p < 0.001$); A_{max} and V_{cmax20} were lower in 2009 than in other years (maximum values of A_{max} and V_{cmax} in 2009 were 26 and 24 % lower than their respective values in 2005).

The dates of the peak values also differed among years. In 2003, the peak value of V_{cmax20} was on DOY 173 in *Q. crispula* shade leaves, but was later in *B. ermanii* leaves (DOY 260) and *Q. crispula* sun leaves (DOY 246). In 2009, the peaks of A_{max} and V_{cmax20} were on DOY 192 in *B. ermanii* leaves, but approximately two months later (on DOY 256) in *Q. crispula* sun leaves (Table 2).

Figure 4 shows the seasonal variations in total leaf nitrogen content (N_{total}) and N_{ph}. N_{total} per unit leaf biomass was high at the start of leaf emergence (ca. 50 mg g^{-1}) and decreased rapidly until mid-June, reaching ca. 20–30 mg g^{-1} (Fig. 4a, b, c). During the summer, N_{total} per unit leaf biomass decreased slowly, and then decreased more rapidly from the end of September. Overall, the N_{total} per unit biomass was similar in the leaves of *B. ermanii* and *Q. crispula* (both sun and shade leaves). The N_{total} per unit leaf area was high in very young leaves (ca. 3–4 g m^{-2}; Fig. 4d, e, f), but showed little variation after early June. In *Q. crispula*, the N_{total} per unit area was lower in shade leaves than in sun leaves.

Both on a leaf biomass and leaf area basis (Fig. 4g, h, i, j, k, l), N_{ph} changed remarkably throughout the season. Both showed a rapid initial increase, a stable period during most of the summer, and a rapid decline in autumn, but the patterns of N_{ph} differed from those of N_{total}. The ratio of N_{ph} to N_{total} was generally low (ca. 10–15 %) at the start of leaf emergence, but increased rapidly to between 40 and 50 % in mid-June (Fig. 4m, n, o). N_{ph}/N_{total} in the sun leaves of *Q. crispula* started to decrease in mid-summer, and the decrease continued through the senescence period, but N_{ph}/N_{total} in *B. ermanii* leaves did not change until leaf fall.

Modeling phenology of leaf characteristics

The seasonal increases in chlorophyll content, A_{max}, V_{cmax20}, J_{max20}, and LMA during the leaf development period fitted well with the development model based on GDD_0. The decline in chlorophyll content, A_{max}, and V_{cmax20} during the autumn senescence period fitted well with the senescence model based on CDD_{18} (Table 3). The senescence model based on CDD_{15} and CDD_{20} showed a poor fit (extremely low r^2 values) with chlo-

Table 4 Fitting parameters (*a*, *b*, *c* and *d*) for logistic models of phenological changes in ecophysiological traits during leaf development period based on growing-degree days above 0 °C (GDD_0; development model) and during senescence period based on chilling-degree days below 18 °C (CDD_{18}; senescence model)

	Development model based on GDD_0				Senescence model based on CDD_{18}			
	a	*b*	*c*	*d*	*a*	*b*	*c*	*d*
Betula ermanii								
Chlorophyll	0	0.48	2.77	0.0052	0	0.48	−5.74	0.0342
A_{max}	0	14.59	4.34	0.0078	0	14.74	−2.60	0.0171
V_{cmax20}	0	47.05	5.30	0.0104	0	43.20	−3.66	0.0209
J_{max20}	0.0002	101.11	7.31	0.0162	–	–	–	–
LMA	0	81.19	0.55	0.0024	–	–	–	–
Quercus crispula (sun leaf)								
Chlorophyll	0	0.58	3.10	0.0047	0	0.58	−2.74	0.0134
A_{max}	0	14.00	3.75	0.0047	0	15.85	−1.46	0.0085
V_{cmax20}	0	47.50	3.50	0.0047	0	47.50	−2.18	0.0097
J_{max20}	0.0002	101.65	3.00	0.0044	0	101.65	−3.67	0.0107
LMA	0.01	100.70	1.18	0.0026	–	–	–	–
Q. crispula (shade leaf)								
Chlorophyll	0	0.50	4.46	0.0072	0	0.50	−4.03	0.0172
A_{max}	0	7.79	10.67	0.0184	0	7.41	−3.09	0.0125
V_{cmax20}	1.50	24.98	9.02	0.0159	0	21.65	−7.26	0.0243
J_{max20}	0	52.62	4.97	0.0100	–	–	–	–
LMA	44.71	17.92	184.07	0.2125	–	–	–	–

A_{max}, light-saturated photosynthetic rate, V_{cmax20} maximum carboxylation rate at 20 °C, J_{max20}, potential electron transport rate at 20 °C, *LMA* leaf mass per unit area

rophyll content and V_{cmax20} of *B. ermanii*. In *Q. crispula* sun leaves, A_{max} and V_{cmax20} fitted the DOY-based model almost as well as the GDD-based model. For all leaves, chlorophyll content and LMA showed a better fit (higher r^2 values) with the GDD_2 model than with the GDD_0 model. For the senescence model, the model based on the opposite value of DOY showed high r^2 values for chlorophyll content of *B. ermanii* and A_{max}, V_{cmax20} and J_{max20} of *Q. crispula* sun leaves. Because LMA showed little change during the senescence period (Fig. 2a, b, c), we did not fit LMA to the senescence model. We did not fit J_{max20} of *B. ermanii* and of *Q. crispula* shade leaves to the senescence model because of insufficient data in October.

We used the developmental model based on GDD_0 and the senescence model based on CDD_{18} (Table 4 and Fig. 5) to clarify the variations in increases and decreases in the ecophysiological parameters of the various species. The maximum values of A_{max}, V_{cmax20}, and J_{max20} were similar in *B. ermanii* and *Q. crispula* sun leaves, and were higher in *B. ermanii* and *Q. crispula* sun leaves than in *Q. crispula* shade leaves. However, the temporal changes in A_{max}, V_{cmax20}, and J_{max20} differed between *B. ermanii* and *Q. crispula*. During the development period, the values of these parameters increased rapidly with increasing GDD_0 in *B. ermanii* sun leaves, but increased more gradually in *Q. crispula* sun leaves (*d* values; Table 4). During the senescence period, A_{max} and V_{cmax} decreased more rapidly in *B. ermanii* leaves than in *Q. crispula* sun leaves. Chlorophyll content also decreased rapidly in *B. ermanii* leaves. These analyses revealed that *B. ermanii* is characterized by rapid growth and senescence, whereas *Q. crispula* is characterized by gradual growth and senescence. In *Q. crispula*, the maximum values of A_{max} and V_{cmax20} were lower, and peaked earlier, in the shade leaves than in the sun leaves (Fig. 5c, e, g).

Relationships among leaf characteristics

To examine the relationships among the leaf morphological and physiological characteristics throughout the growing season (i.e., as a function of leaf age), we further analyzed the data by dividing the leaves into three age classes according to DOY: young leaves (DOY ≤ 160), mature leaves (160 < DOY ≤ 240), and senescing leaves (240 < DOY). This classification relates to apparent changes in physiological activities: DOY 160 corresponds to the timing of the sharp change in the seasonal curve for dark respiration (R_{20}; Fig. 3a, b, c), and DOY 240 corresponds to the point when A_{max} begins to decrease from its maximum level as a result of senescence (Fig. 3d, e, f).

In all of the leaves, there were strong and statistically significant positive linear correlations between J_{max} and V_{cmax} (both at measured temperatures) throughout the season, indicating that these parameters changed in the same manner from leaf expansion to maturity and from maturity to senescence (Table 3; Fig. 6). The slopes of the relationships between J_{max} and V_{cmax} (i.e., the ratio of J_{max} to V_{cmax}) were steeper for the young and senescing leaves than for the mature leaves (Fig. 6d, e, f), indicating that J_{max}/V_{cmax} changed in the middle of the growing season.

Chlorophyll content and V_{cmax20} were also significantly positively correlated throughout the growing

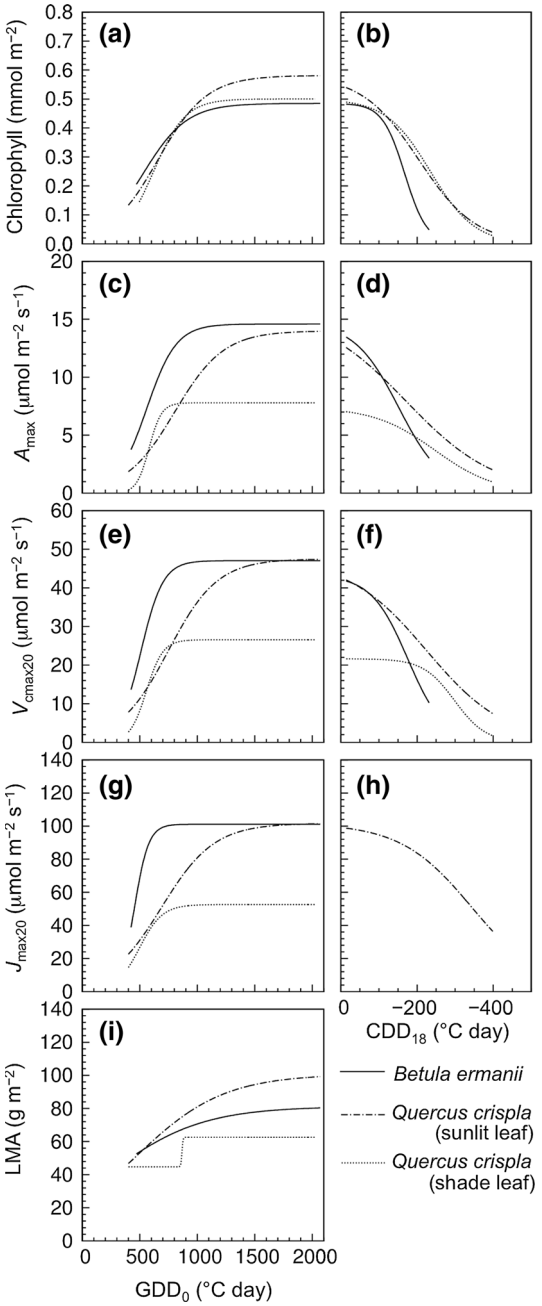

Fig. 5 Logistic models during leaf development period for **a** chlorophyll content, **c** light-saturated photosynthesis (A_{max}), **e** maximum carboxylation rate at 20 °C (V_{cmax20}), **g** potential electron transport rate at 20 °C (J_{max20}), and (i) leaf mass per unit area (LMA) based on growing-degree days above 0 °C (GDD_0) and corresponding values during senescence period for **b** chlorophyll content, **d** A_{max}, **f** V_{cmax20}, and **h** J_{max20} based on chilling-degree days below 18 °C (CDD_{18}). Fitting parameters are provided in Table 4

season (Table 5; Fig. 7a, b, c). V_{cmax20} and LMA were significantly positively correlated for all leaf-age groups of *B. ermanii* leaves and *Q. crispula* sun leaves, but there was no significant correlation between V_{cmax20} and LMA for *Q. crispula* shade leaves (Table 3; Fig. 7d, e, f). In the young and mature leaves, V_{cmax20} was correlated less strongly with LMA in *B. ermanii* sun leaves ($r^2 = 0.38$, $P < 0.001$) than in *Q. crispula* sun leaves ($r^2 = 0.63$, $P < 0.001$). Throughout the growing season, V_{cmax20} was only significantly correlated with N_{total} per unit leaf area in *B. ermanii* leaves and *Q. crispula* sun leaves (Table 3, Fig. 7g, h). In mature and senescing leaves, the correlations between V_{cmax20} and N_{total} per unit leaf area were weaker in *B. ermanii* leaves ($r^2 = 0.44$, $P < 0.001$) than in *Q. crispula* sun leaves ($r^2 = 0.60$, $P < 0.001$), but both correlations were stronger than that in *Q. crispula* shade leaves ($r^2 = 0.38$, $P < 0.001$).

Chlorophyll content was significantly positively correlated with N_{total} per unit leaf area in all leaves throughout the growing season (Table 3). The strongest correlation (highest r^2 value) was for *Q. crispula* sun leaves (Table 3; Fig. 7k), which might have resulted from a lack of chlorophyll data for some of the sampled leaves (i.e., values with a high N_{total} per unit leaf area and low V_{cmax20} in Fig. 7h). We could not obtain chlorophyll data for these very young leaves because they were too small to obtain enough leaf material for chlorophyll analyses after the photosynthetic measurements. If we only analyze the data for the mature and senescing leaves, the chlorophyll content was strongly positively correlated with N_{total} per unit leaf area in *B. ermanii* leaves ($r^2 = 0.46$, $P < 0.001$) and in *Q. crispula* sun leaves ($r^2 = 0.61$, $P < 0.001$) and shade leaves ($r^2 = 0.31$, $P < 0.001$).

Discussion

Seasonal and interannual variations in ecophysiological characteristics

Our goal in this long-term ecophysiological research on tree leaf morphology and physiology is to obtain essential information on the leaf-level characteristics that are responsible for the spatial and temporal dynamics of CO_2 fluxes in a deciduous broadleaf forest canopy. In a previous study (Muraoka and Koizumi 2005), we found that *B. ermanii* and *Q. crispula* showed remarkable seasonal changes in their photosynthetic capacity and stomatal conductance, and we recognized that leaf phenology must be a fundamental ecological process affecting ecosystem-scale photosynthetic productivity in deciduous forests (see also Wilson et al. 2001). In previous studies on the canopy leaf area index, we revealed the phenology of leaf and canopy structure and functions by investigating the seasonal changes in single-leaf area and canopy-level leaf biomass (Nasahara et al. 2008). We have also estimated ecosystem-level carbon budgets using simulation models (Ito et al. 2006; Muraoka et al. 2010).

The present study was based on 5–7 years of data, although the measurements are continuing. Our analyses show that there were interannual variations in the timings of leaf maturation and senescence (Figs. 2, 3). The

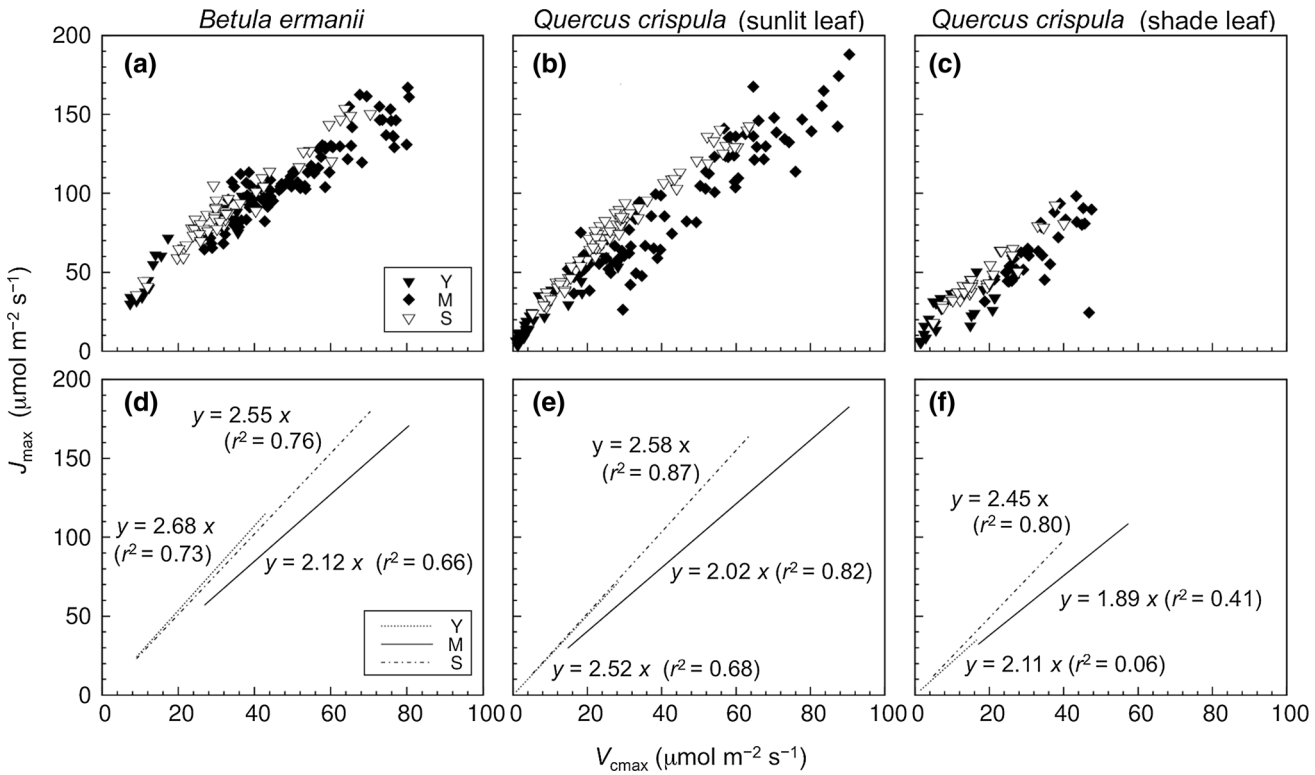

Fig. 6 Relationships between maximum carboxylation rate (V_{cmax}) and potential electron transport rate (J_{max}). Leaves were divided into three leaf-age groups (*Y* young, *M* mature, *S* senescing) according to day of year (DOY) when the trend for certain parameters changed (see text for details). Linear regressions between J_{max} and V_{cmax} for each leaf age group are shown in *lower panels* (**d**, **e**, **f**) along with *slope* of each line. Results for linear regressions for the entire growing season are shown in Table 5

A_{max} values varied by approximately 25 % among years (Fig. 3), although this forest is not subject to drought, unlike many temperate North American forests (Abrams and Mostoller 1995; Wilson et al. 2001; Xu and Baldocchi 2003). The Takayama forest site is in the Asian monsoon region, so it receives sufficient precipitation throughout the growing season (Table 1). Wang et al. (2008) investigated the leaf photosynthetic capacity, nitrogen content, and LMA of *Fagus crenata* Blume along an elevation gradient on a mountain in a cool-temperate region of Japan, and found that its leaf characteristics showed interannual variations from 2000 to 2005.

The multi-year measurements in this study revealed clear interspecific differences in the phenological patterns of ecophysiological properties between *B. ermanii* and *Q. crispula*, even though both species belong to the same functional type (here, deciduous broadleaf trees). The seasonal increases in A_{max}, V_{cmax}, and J_{max} and decreases in A_{max} and V_{cmax} occurred more rapidly in *B. ermanii* leaves than in *Q. crispula* sun leaves (Figs. 3, 5, 6). For both species, these characteristics were successfully described by our phenology model based on a logistic equation that included cumulative air temperature (GDD and CDD) as the independent variable (Fig. 5). In *B. ermanii*, the increases in photosynthetic parameters during the leaf development period fitted better with the logistic model based on GDD than with that based on calendar date (DOY). This was because the timings of leaf budbreak differed among the years due to differences in air temperatures during the spring (Table 1). In *Q. crispula* sun leaves, the development of A_{max} and V_{cmax} were explained equally well by the DOY-based model and the GDD_0-based model. In another study at the same forest site, the yearly variations in GDD_2 and CDD_{18} strongly affected the timings of the start of leaf-expansion and the end of leaf-fall, as estimated from digital camera images (Nagai et al. 2013). The findings of that study are consistent with our findings that the development of chlorophyll content and LMA showed the best fit with the GDD_2-based model, and the decrease in chlorophyll content during senescence showed the best fit with the CDD_{18}-based model (Table 3). Several other studies have reported interspecific variations in the seasonal patterns of leaf ecophysiological variables (Reich et al. 1991; Wilson et al. 2000; Niinemets et al. 2004). To better understand the phenology of these physiological traits, it may be insufficient to consider only the functional type of the tree.

Another interesting finding was the interannual variations in leaf phenology. The irregular patterns of photosynthetic capacity in the summers of 2003 and 2009 (Fig. 3; Table 2) might be caused by the rainy season (“baiu”). In 2003, the meteorological conditions

Table 5 Linear regression coefficients between primary photosynthetic parameters and leaf characteristics

Dependent value	Independent value	Intercept	Slope	r^2	P	N
Betula ermanii						
J_{max}	V_{cmax}	32.49	1.57	0.89	< 0.001	172
V_{cmax20}	Chlorophyll	13.37	61.76	0.44	< 0.001	149
V_{cmax20}	LMA	13.59	0.35	0.11	< 0.001	174
V_{cmax20}	N_{total}/area	26.07	6.71	0.06	0.004	148
Chlorophyll	N_{total}/area	0.18	0.11	0.12	< 0.001	138
Quercus crispula (sun leaf)						
J_{max}	V_{cmax}	17.80	1.79	0.90	< 0.001	199
V_{cmax20}	Chlorophyll	3.73	66.13	0.59	< 0.001	164
V_{cmax20}	LMA	−6.38	0.42	0.32	< 0.001	184
V_{cmax20}	N_{total}/area	5.63	13.20	0.26	< 0.001	161
Chlorophyll	N_{total}/area	−0.13	0.29	0.56	< 0.001	145
Q. crispula (shade leaf)						
J_{max}	V_{cmax}	13.17	1.57	0.77	< 0.001	96
V_{cmax20}	Chlorophyll	4.30	43.87	0.63	< 0.001	78
V_{cmax20}	LMA	11.49	0.14	0.03	0.086	94
V_{cmax20}	N_{total}/area	20.22	0.38	0.0005	0.847	73
Chlorophyll	N_{total}/area	0.04	0.24	0.22	< 0.001	54

J_{max} potential electron transport rate, V_{cmax} maximum carboxylation rate, V_{cmax20} V_{cmax} at 20 °C, *chlorophyll* total chlorophyll content, *LMA* leaf mass per unit area, N_{total} total nitrogen content per unit leaf area

on the main island of Japan were characterized by remarkable decrease in incident radiation due to thick cloud cover during the baiu (Japan Meteorological Agency 2005), resulting in a lower mean air temperature in July than in the other years (Table 1). In 2009, the end date of the baiu was the latest recorded from 1951 to 2014 (Japan Meteorological Agency 2014), and the number of sunshine hours during July was about half that in normal years (Japan Meteorological Agency 2009). Since leaf photosynthetic development responds to PPFD (Niinemets et al. 2004) and temperature, the sunlight shortage and lower temperatures might have delayed the photosynthetic development of *B. ermanii* and *Q. crispula* leaves at the Takayama site. Saigusa et al. (2008) discussed the effects of the sunlight shortage in 2003 on forest-level CO_2 uptake in Asia, and found that this sunlight anomaly affected gross primary production at the Takayama site.

It is unclear why the chlorophyll content of *B. ermanii* leaves was markedly lower in 2006 than in other years (Fig. 2d). This phenomenon was not apparent for the sun leaves of *Q. crispula* (Fig. 2e). Various factors that we did not examine (e.g., frost in the early spring, herbivory, pathogens) could have affected the biochemical properties of *B. ermanii* leaves.

Comparison of the sun and shade leaves of *Q. crispula* provided additional ecologically important information about the multi-layered canopy at the study site. The timings of leaf budbreak of *Q. crispula* in sunlit and shaded environments were similar in all years. The photosynthetic capacity of the sun and shade leaves increased in a similar manner from leaf budbreak (around DOY 140) to DOY 180. Then, the photosynthetic capacity reached its maximum in the shade leaves but continued to increase in the sun leaves (Fig. 3e, f), resulting in higher maximum capacity in the sun leaves and faster maturation of the shade leaves (Fig. 5). The light availability (relative PPFD) to the shade leaves in the crown of *Q. crispula* was almost at the seasonal minimum at around DOY 180, and this could have affected the development of shade leaves as they acclimated to the low-light environment (see also Niinemets et al. 2004).

Seasonal changes in leaf morphological, photosynthetic, and nitrogen-use characteristics

Our measurements during the 7 years revealed details of the seasonal changes in chlorophyll and nitrogen contents, photosynthetic parameters, dark respiration, and leaf morphology (LMA), as well as their interactions. In general, leaf photosynthetic capacity is proportional to leaf nitrogen content (Hikosaka 2004), and their relationship has been widely examined for leaves from various species in a range of biomes around the world (e.g., Wright et al. 2004). The strength of the relationship between photosynthetic capacity and leaf nitrogen content has been examined for a wide range of plant species including herbaceous and trees (e.g., Evans 1989; Reich et al. 1994, 1995). The results of such studies have provided a deeper understanding of nitrogen use during photosynthesis (Hikosaka 2004).

Most studies have focused on mature leaves, but analyses of developing and senescing leaves can increase our understanding of leaf phenology. In developing or senescing leaves, there are changes in leaf structural and biochemical components that are tightly linked. These changes reflect the anatomical and physiological responses to a fluctuating environment, as well as the resource acquisition and use strategies of a species throughout the growing season (cf. Marshall and Roberts 2000). Reich et al. (1991) and Wilson et al. (2000) have shown in maple (*Acer* spp.) and oak (*Quercus* spp.)

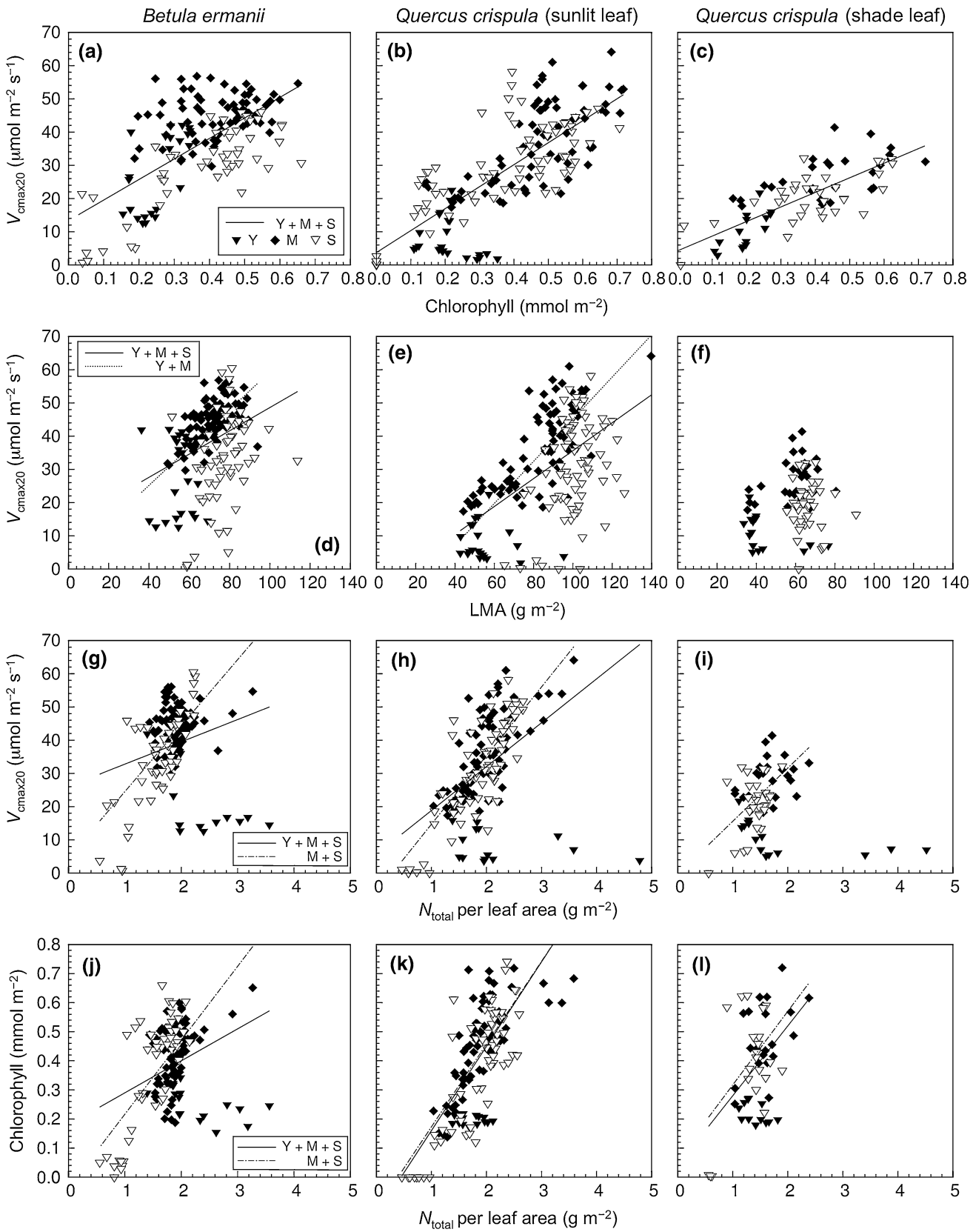

Fig. 7 Relationships between (a, b, c) maximum carboxylation rate at 20 °C (V_{cmax20}) and chlorophyll content, **d**, **e**, **f** V_{cmax20} and leaf mass per unit area (LMA), **g**, **h**, **i** V_{cmax20} and total nitrogen (N_{total}) per unit leaf area, and **j**, **k**, **l** chlorophyll content and N_{total} per unit leaf area. Leaves were divided into three leaf-age groups (*Y* young, *M* mature, *S* senescing) according to day of year (DOY) when the trend for certain parameters changed (see text for details). *Regression lines* are shown for statistically significant relationships (see Table 5)

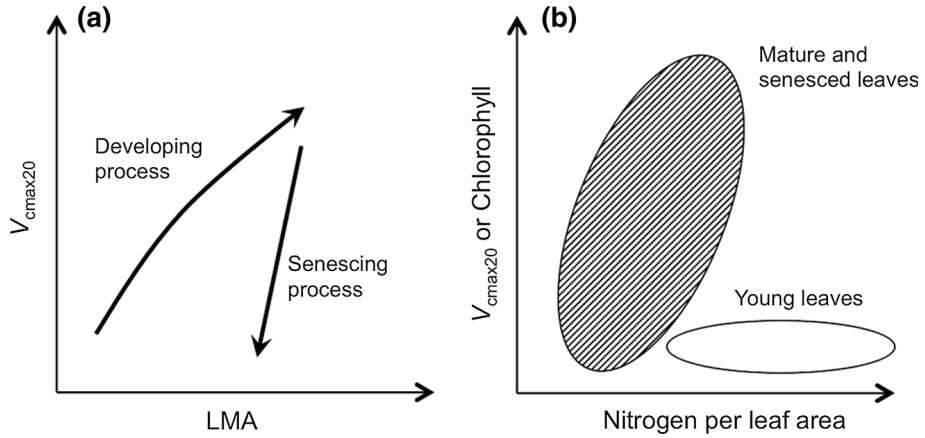

Fig. 8 Conceptual diagrams showing seasonal variations in relationships between **a** maximum carboxylation rate at 20 °C (V_{cmax20}) and leaf mass per unit area (LMA) and **b** V_{cmax20} or chlorophyll content and total nitrogen (N_{total}) per unit leaf area

that the leaf nitrogen content and photosynthetic capacity, and their relationship, change during the growing season (i.e., as the leaves age). Miyazawa et al. (1998) and Yasumura and Ishida (2011) have shown that for evergreen broadleaf tree leaves, the relationship between leaf nitrogen and photosynthetic capacity (and, in turn, nitrogen use efficiency) changes as the leaves age. In *B. ermanii* and *Q. crispula* trees at the Takayama site, the leaf morphological and biochemical parameters showed rapid changes during the development of young leaves, relatively stable values in mature leaves, and decreasing values in senescing leaves (Figs. 2, 3, 4). However, the phenology of LMA, nitrogen content, and photosynthetic capacity did not always change in the same way, and so the relationships among these characteristics changed as the leaves aged.

Figure 8a illustrates the relationship between LMA and photosynthetic capacity in *B. ermanii* and *Q. crispula*. From leaf expansion to maturity (i.e., during the leaf development process), LMA and photosynthetic capacity increased proportionally. However, by late summer or autumn, the photosynthetic capacity decreased rapidly (i.e., during senescence) while LMA remained relatively constant. Thus, the relationship between V_{cmax} and LMA showed a pattern of hysteresis during these two parts of the growing season (Fig. 7). Similar hysteresis was reported by Reich et al. (1991) in oak (*Quercus ellipsoidalis*) and maple (*Acer rubrum* and *A. saccharum*).

The seasonal changes in R_{20} also reflected the leaf developmental stage (Fig. 3a, b, c). In young leaves, R_{20} was very high and then decreased rapidly. The respiration rate consists of two components: maintenance respiration, which is associated with energy generation and metabolic processes and is proportional to the amount of biomass; and growth (construction) respiration, which is associated with the construction of plant tissues (Amthor 1989). The high R_{20} during the very early growing season probably reflects the high growth component of respiration during leaf development.

Figure 8b illustrates the relationship between the nitrogen content per unit leaf area and photosynthetic capacity. In the early growing season, there was a high nitrogen content (Fig. 4a, b, c, d, e, f) but a low chlorophyll content (Fig. 2d, e, f). At this stage, the photosynthetic capacity had not yet fully developed (Fig. 3d, e, f, g, h, i, j, k, l), leading to a poor correlation between N_{total} per unit area and photosynthetic capacity (young leaves in Fig. 8b). As the chlorophyll content and photosynthetic capacity increased, the relationship became more proportional (mature and senescing leaves in Fig. 8b). Reich et al. (1991) reported a similar relationship between leaf nitrogen content and photosynthetic capacity, and Wilson et al. (2000) and Wang et al. (2008) reported that the relationship between V_{cmax} and N_{total} per unit area was strongest in spring and early summer, and became weaker thereafter.

Implications for ecosystem-scale research in time and space

In large-scale ecosystem research such as carbon cycle models or remote sensing-based models, seasonal changes in leaf biochemical and photosynthetic characteristics are generally ignored or are regarded as the same as seasonal changes in leaf area (e.g., Bonan 1995; but see Ito et al. 2006). However, our analyses indicate that the phenology of leaf characteristics can affect the analyses and predictions of forest-scale photosynthetic productivity and the resulting carbon balance in deciduous forests in temperate regions, as reported in previous studies (Wilson et al. 2001; Ito et al. 2006; Muraoka et al. 2010, 2013).

In this study, we successfully described the seasonal changes of leaf ecophysiological characteristics as a function of cumulative air temperature, during both leaf development (GDD) and leaf senescence (CDD). Many studies on leaf phenology have attempted to explain interannual variations and geographical differences in phenological events based on the calendar date. This is

logical, because leaf development is considered to be triggered by certain temperature conditions or by thermal accumulation (Chuine et al. 2003; Hänninen and Tanino 2011). As mentioned above, the long rainy season in the summer of 2003 may have delayed leaf photosynthetic development as a result of the lower temperatures during July of that year. Although PPFD and soil water availability must also be considered, at least for deciduous trees in temperate regions, the results of the present study show that it should be possible to predict the development of leaf ecophysiological characteristics as a function of GDD.

The environmental factors that influence leaf senescence have not yet been unequivocally defined (Schaber and Badeck 2003). More detailed analyses are required to develop a leaf senescence model based on physiological mechanisms. In this study, senescence was successfully fitted to a simple logistic model based on CDD as the independent variable. Our empirical phenological models for leaf ecophysiological characteristics could be incorporated in plant growth, ecosystem carbon cycle, and hydrological models, thereby improving future analyses of the functional roles of canopy processes in growth, carbon cycling, and hydrology. This will also improve predictions of forest ecosystem function under future climate change scenarios. Currently, we are conducting an open-field experiment in which we are warming the upper branches of *Q. crispula* and *B. ermanii* to examine the possible effects of global warming on leaf morphology, photosynthesis, and phenology (Chung et al. 2013).

Another contribution of ecophysiological research on forest leaf phenology is to improve the ecophysiological uses of remote sensing data (Muraoka and Koizumi 2009). Recently, researchers have attempted to observe the seasonal changes in the ecophysiological status of a forest canopy using indirect methods such as in situ and satellite remote sensing (Nishida 2007; Muraoka et al. 2013) and digital camera images (Richardson et al. 2007; Ahrends et al. 2009; Nagai et al. 2013). The spectral reflectance of the canopies measured by spectroradiometers and RGB signals recorded by a digital camera can reflect the leaf anatomical, biochemical, and photosynthetic properties of the forest canopy. However, to improve the accuracy of monitoring the spatial and temporal dynamics of forest canopies via remote sensing, a more comprehensive understanding of the relationships among plant morphological and biochemical structures and optical signals (reflectance, RGB signals) is required. In the present study, we found that the chlorophyll content was strongly correlated with V_{cmax}. This is an important finding, because the leaf chlorophyll content strongly affects the optical characteristics of the leaves (Porra et al. 1989; Gitelson et al. 1996; Sims and Gamon 2002). Our findings suggest that it may be possible to estimate the spatial distribution and temporal changes of ecosystem-level photosynthetic capacity from optical remote sensing data. Indeed, an optical index for canopy chlorophyll content obtained by in situ remote sensing was found to be strongly correlated with the daily maximum gross primary production of the canopy from the leaf expansion period to maturity and senescence in multiple years (Muraoka et al. 2013). Further integrated studies of leaf- and canopy-level ecophysiology, combined with process-based models and optical remote sensing at monitoring sites, promise to support and improve analyses of the environmental response of terrestrial ecosystems to climate change.

Acknowledgments We thank K. Kurumado, M. Ohno, Y. Miyamoto, and Y. Hiomo of the Takayama field station, Gifu University, and the "Takayama Community" members, especially S. Yamamoto and H. Kondo of the National Institute of Advanced Industrial Science and Technology, A. Ito of the National Institute for Environmental Studies, T. Akiyama of Gifu University, T. Hiura of Hokkaido University, and J. D. Tenhunen of the University of Bayreuth, for their support during our field measurements and for encouragement during this long-term research. We also thank S. Kinoshita, Center for Environmental Measurement and Analysis, National Institute for Environmental Studies, for leaf nitrogen analyses. We thank the anonymous reviewers for their constructive comments on this manuscript. This long-term ecological research was supported by the Ministry of the Environment, Japan, as a Global Environment Research Fund project (S-1, PI: T. Oikawa). This work was also supported by the Japan Society for the Promotion of Science (JSPS) 21st Century COE Program (Satellite Ecology) at Gifu University, KAKENHI (JSPS grant no. 18710006 to HM), the JSPS-NRF-NSFC A3 Foresight Program (PI: H. Muraoka), the Environment Research and Technology Development Fund of the Ministry of Environment, Japan (D-0909, PI: T. Hiura), the Global Change Observation Mission of the Japan Aerospace Exploration Agency (PI#102), and the JSPS Funding Program for Next Generation World-Leading Researchers (to HM).

References

Abrams MD, Mostoller SA (1995) Gas exchange, leaf structure and nitrogen in contrasting successional tree species growing in open and understory sites during a drought. Tree Physiol 15:361–370

Ahrends HE, Etzold S, Kutsch WL, Stoeckli R, Bruegger R, Jeanneret F, Wanner H, Buchmann N, Eugster W (2009) Tree phenology and carbon dioxide fluxes: use of digital photography for process-based interpretation at the ecosystem scale. Clim Res 39:261–274

Amthor JS (1989) Respiration and crop productivity. Springer, New York

Augspurger CK (2008) Early spring leaf out enhances growth and survival of saplings in a temperate deciduous forest. Oecologia 156:281–286

Baldocchi D, Meyers T (1998) On using eco-physiological, micrometeorological and biogeochemical theory to evaluate carbon dioxide, water vapor and trace gas fluxes over vegetation: a perspective. Agr Forest Meteorol 90:1–25

Baldocchi D, Falge E, Gu L, Olson R, Hollinger D, Running S, Anthoni P, Bernhofer C, Davis K, Evans R, Fuentes J, Goldstein A, Katul G, Law B, Lee X, Malhi Y, Meyers T, Munger W, Oechel W, Paw UKT, Pilegaard K, Schmid HP, Valentini R, Verma S, Vesala T, Wilson K, Wofsy S (2001) FLUXNET : a new tool to study the temporal and spatial variability of ecosystem-scale carbon dioxide, water vapor, and energy flux densities. B Am Meteorol Soc 82:2415–2434

Beer C, Reichstein M, Tomelleri E, Ciais P, Jung M, Carvalhais N, Rödenbeck R, Arain MF, Baldocchi D, Bonan GB, Bondeau A, Cescatti A, Lasslop G, Lindroth A, Lomas M, Luyssaert S, Margolis H, Oleson KW, Roupsard O, Veenendaal E, Viovy N,

Williams C, Papale D (2010) Terrestrial gross carbon dioxide uptake: global distribution and covariation with climate. Science 329:834–838
Bernacchi CJ, Singsaas EL, Pimentel C, Portis AR, Long SP (2001) Improved temperature response functions for models of Rubisco-limited photosynthesis. Plant Cell Environ 24:253–259
Bernacchi CJ, Bagley JE, Serbin SP, Ruiz-Vera UM, Rosenthal DM, Vanloocke A (2013) Modelling C_3 photosynthesis from the chloroplast to the ecosystem. Plant, Cell Environ 36:1641–1657
Bonan GB (1995) Land-atmosphere interactions for climate system models: coupling biophysical, biogeochemical, and ecosystem dynamical processes. Remote Sens Environ 51:57–73
Bonan GB (1996) A land surface model (LSM version 1.0) for ecological, hydrological, and atmospheric studies: technical description and user's guide. National Center for Atmospheric Research, Boulder
Canadell JG, Raupach MR (2008) Managing forests for climate change mitigation. Science 320:1456–1457
Canadell JG, Mooney HA, Baldocchi DD, Berry JA, Ehleringer JR, Field CB, Gower ST, Hollinger DY, Hunt JE, Jackson RB, Running SW, Shaver GR, Steffen W, Trumbore SE, Valentini R, Bond BY (2000) Carbon metabolism of the terrestrial biosphere: a multi technique approach for improved understanding. Ecosystems 3:115–130
Chmielewski F, Rötzer T (2002) Annual and spatial variability of the beginning of growing season in Europe in relation to air temperature changes. Clim Res 19:257–264
Chuine I, Kramer K, Hänninen H (2003) Plant development models. In: Schwartz MD (ed) PHENOLOGY: an integrative environmental science. Kluwer Academic Publishers, Dordrecht, pp 217–235
Chung H, Muraoka H, Nakamura M, Han S, Muller O, Son Y (2013) Experimental warming studies on tree species and forest ecosystems: a literature review. J Plant Res 126:447–460
Cleland EE, Chuine I, Menzel A, Mooney HA, Schwartz MD (2007) Shifting plant phenology in response to global change. Trends Ecol Evol 22:357–365
Evans J (1989) Photosynthesis and nitrogen relationships in leaves of C_3 plants. Oecologia 78:9–19
Fang J, Guo Z, Hu H, Kato T, Muraoka H, Son Y (2014) Forest biomass carbon sinks in East Asia, with special reference to the relative contributions of forest expansion and forest growth. Glob Change Biol 20:2019–2030
Farquhar G, von Caemmerer S, Berry J (1980) A biochemical model of photosynthetic CO_2 assimilation in leaves of C_3 species. Planta 149:78–90
Gitelson AA, Merzlyak MN, Lichtenthaler HK (1996) Detection of red edge position and chlorophyll content by reflectance measurements near 700 nm. J Plant Physiol 148:501–508
Goulden ML, Munger JW, Fan SM, Daube BC, Wofsy SC (1996) Exchange of carbon dioxide by a deciduous forest: response to interannual climate variability. Science 271:1576–1578
Hänninen H, Tanino K (2011) Tree seasonality in a warming climate. Trends Plant Sci 16:412–416
Harley P, Baldocchi D (1995) Scaling carbon dioxide and water vapour exchange from leaf to canopy in a deciduous forest. I. Leaf model parameterization. Plant Cell Environ 18:1146–1156
Hikosaka K (2004) Interspecific difference in the photosynthesis-nitrogen relationship: patterns, physiological causes, and ecological importance. J Plant Res 117:481–494
Hikosaka K, Terashima I (1995) A model of the acclimation of photosynthesis in the leaves of C_3 plants to sun and shade with respect to nitrogen use. Plant Cell Environ 18:605–618
Hikosaka K, Nabeshima E, Hiura T (2007) Seasonal changes in the temperature response of photosynthesis in canopy leaves of *Quercus crispula* in a cool-temperate forest. Tree Physiol 27:1035–1041
Ide R, Oguma H (2010) Use of digital cameras for phenological observations. Ecological Inform 5:339–347
Ito A (2008) The regional carbon budget of East Asia simulated with a terrestrial ecosystem model and validated using AsiaFlux data. Agr For Meteorol 148:738–747
Ito A, Oikawa T (2002) A simulation model of the carbon cycle in land ecosystems (Sim-CYCLE): a description based on dry-matter production theory and plot-scale validation. Ecol Model 151:143–176
Ito A, Muraoka H, Koizumi H, Saigusa N, Murayama S, Yamamoto S (2006) Seasonal variation in leaf properties and ecosystem carbon budget in a cool-temperate deciduous broad-leaved forest: simulation analysis at Takayama site, Japan. Ecol Res 21:137–149
Japan Meteorological Agency (2005) Report on abnormal weather 2005. http://www.data.jma.go.jp/cpdinfo/climate_change/2005/pdf/2005_all.pdf (in Japanese; accessed May 31, 2014)
Japan Meteorological Agency (2009) The climate in July. http://www.data.jma.go.jp/obd/stats/data/stat/tenko0907.pdf (in Japanese; accessed September 24, 2014)
Japan Meteorological Agency (2014) The start and end date of the baiu from 1951: Tokai region. http://www.data.jma.go.jp/fcd/yoho/baiu/kako_baiu08.html (in Japanese; accessed September 24, 2014)
Keeling C, Chin J, Whorf T (1996) Increased activity of northern vegetation inferred from atmospheric CO_2 measurements. Nature 382:146–149
Koike T (1988) Leaf structure and photosynthetic performance as related to the forest succession of deciduous broad-leaved trees. Plant Species Biol 3:77–87
Kosugi Y, Shibata S, Kobashi S (2003) Parameterization of the CO_2 and H_2O gas exchange of several temperate deciduous broad-leaved trees at the leaf scale considering seasonal changes. Plant, Cell Environ 26:285–301
Kramer K, Leinonen I, Loustau D (2000) The importance of phenology for the evaluation of impact of climate change on growth of boreal, temperate and Mediterranean forests ecosystems: an overview. Int J Biometeorol 44:67–75
Marshall B, Roberts JA (2000) Leaf development and canopy growth. Sheffield Academic Press, Sheffield
Medlyn B, Dreyer E, Ellsworth D, Forstreuter M, Harley PC, Kirschbaum MUF, Le Roux X, Montpied P, Strassemeyer J, Walcroft A, Wang K, Loustau D (2002) Temperature response of parameters of a biochemically based model of photosynthesis. II. A review of experimental data. Plant Cell Environ 25:1167–1179
Menzel A, Sparks TH, Estrella N, Koch E, Aasa A, Ahas R, Alm-kübler K, Bissolli P, Braslavská O, Briede A, Chmielewski FM, Crepinsek Z, Curnel Y, Dahl Å, Defila C, Donnelly A, Filella Y, Jatczak K, Måge F, Mestre A, Nordli Ø, Peñuelas J, Pirinen P, Remišová V, Scheifinger H, Striz M, Susnik A, Van Vliet AJH, Wielgolaski F, Zach S, Zust A (2006) European phenological response to climate change matches the warming pattern. Glob Change Biol 12:1969–1976
Miyazawa S, Satomi S, Terashima I (1998) Slow leaf development of evergreen broad-leaved tree species in Japanese warm temperate forests. Ann Bot London 82:859–869
Mo W, Lee MS, Uchida M, Inatomi M, Saigusa N, Mariko S, Koizumi H (2005) Seasonal and annual variations in soil respiration in a cool-temperate deciduous broad-leaved forest in Japan. Agr For Meteorol 134:81–94
Morin X, Roy J, Sonié L, Chuine I (2010) Changes in leaf phenology of three European oak species in response to experimental climate change. New Phytol 186:900–910
Muraoka H, Koizumi H (2005) Photosynthetic and structural characteristics of canopy and shrub trees in a cool-temperate deciduous broadleaved forest: implication to the ecosystem carbon gain. Agr For Meteorol 134:39–59
Muraoka H, Koizumi H (2009) Satellite Ecology (SATECO)-linking ecology, remote sensing and micrometeorology, from plot to regional scale, for the study of ecosystem structure and function. J Plant Res 122:3–20
Muraoka H, Saigusa N, Nasahara KN, Noda H, Yoshino J, Saitoh TM, Nagai S, Koizumi H (2010) Effects of seasonal and interannual variations in leaf photosynthesis and canopy leaf area index on gross primary production of a cool-temperate deciduous broadleaf forest in Takayama, Japan. J Plant Res 123:563–576

Muraoka H, Noda HM, Nagai S, Motohka T, Saitoh TM, Nasahara KN, Saigusa N (2013) Spectral vegetation indices as the indicator of canopy photosynthetic productivity in a deciduous broadleaf forest. J Plant Ecol 6:393–407

Murayama S, Takamura C, Yamamoto S, Saigusa N, Morimoto S, Kondo H, Nakazawa T, Aoki S, Usami T, Kondo M (2010) Seasonal variations of atmospheric CO_2, $\delta^{13}C$, and δ^{18} O at a cool temperate deciduous forest in Japan: influence of Asian monsoon. J Geophys Res 115(D17):D17304

Myneni R, Keeling C, Tucker C (1997) Increased plant growth in the northern high latitudes from 1981 to 1991. Nature 386:698–702

Nagai S, Nasahara KN, Muraoka H, Akiyama T, Tsuchida S (2010) Field experiments to test the use of the normalized difference vegetation index for phenology detection. Agr For Meteorol 150:152–160

Nagai S, Saitoh TM, Kurumado K, Tamagawa I, Kobayashi H, Inoue T, Suzuki R, Gamo M, Muraoka H, Nasahara NK (2013) Detection of bio-meteorological year-to-year variation by using digital canopy surface images of a deciduous broadleaved forest. SOLA 9:106–110

Nakaji T, Ide R, Oguma H, Saigusa N, Fujinuma Y (2007) Utility of spectral vegetation index for estimation of gross CO_2 flux under varied sky conditions. Remote Sens Environ 109:274–284

Nasahara KN, Muraoka H, Nagai S, Mikami H (2008) Vertical integration of leaf area index in a Japanese deciduous broadleaved forest. Agr For Meteorol 148:1136–1146

Niinemets Ü, Tenhunen JD (1997) A model separating leaf structural and physiological effects on carbon gain along light gradients for the shade-tolerant species *Acer saccharum*. Plant Cell Environ 20:845–866

Niinemets Ü, Kull O, Tenhunen J (2004) Within-canopy variation in the rate of development of photosynthetic capacity is proportional to integrated quantum flux density in temperate deciduous trees. Plant Cell Environ 27:293–313

Nishida K (2007) Phenological eyes network (PEN)—A validation network for remote sensing of the terrestrial ecosystems. Asia-Flux Newslett 21:9–13

Ohtsuka T, Akiyama T, Hashimoto Y, Inatomi M, Sakai T, Jia S, Mo W, Tsuda S, Koizumi H (2005) Biometric based estimates of net primary production (NPP) in a cool-temperate deciduous forest stand beneath a flux tower. Agr For Meteorol 134:27–38

Ohtsuka T, Mo W, Satomura T, Inatomi M, Koizumi H (2007) Biometric based carbon flux measurements and net ecosystem production (NEP) in a temperate deciduous broad-leaved forest beneath a flux tower. Ecosystems 10:324–334

Ohtsuka T, Saigusa N, Koizumi H (2009) On linking multiyear biometric measurements of tree growth with eddy covariance-based net ecosystem production. Glob Change Biol 15:1015–1024

Owen KE, Tenhunen J, Reichstein M, Wang Q, Falge E, Geyer R, Xiao X, Stoy P, Ammann C, Arain A, Aubinet M, Aurela M, Bernhofer C, Chojnicki BH, Granier A, Gruenwald T, Hadley J, Heinesch B, Hollinger D, Knoh A, Kutsch W, Lohila A, Meyers T, Moors E, Moureaux C, Pilegaard K, Saigusa N, Verma S, Vesala T, Vogel C (2007) Linking flux network measurements to continental scale simulations: ecosystem carbon dioxide exchange capacity under non-water-stressed conditions. Glob Change Biol 13:734–760

Peñuelas J, Rutishauser T, Filella I (2009) Phenology feedbacks on climate change. Science 324:887–888

Piao S, Fang J, Zhou L, Ciais P, Zhu B (2006) Variations in satellite-derived phenology in China's temperate vegetation. Glob Change Biol 12:672–685

Piao S, Ciais P, Friedlingstein P, Peylin P, Reichstein M, Luyssaert S, Margolis H, Fang J, Barr A, Chen A, Grelle A, Hollinger DY, Laurila T, Lindroth A, Richardson AD, Vesala T (2008) Net carbon dioxide losses of northern ecosystems in response to autumn warming. Nature 451:49–52

Piao S, Ito A, Li S, Huang Y, Ciais P, Wang X, Peng S, Andres RJ, Fang J, Jeong S, Mao J, Mohammat A, Muraoka H, Nan H, Peng C, Peylin P, Shi X, Sitch S, Tao S, Tian H, Xu M, Yu G, Zeng N, Zhu B (2012) The carbon budget of terrestrial ecosystems in East Asia over the last two decades. Biogeosci Discuss 9:4025–4066

Porra R, Thompson W, Kriedemann P (1989) Determination of accurate extinction coefficients and simultaneous equations for assaying chlorophylls a and b extracted with four different solvents: verification of the concentration of chlorophyll standards by atomic absorption spectroscopy. Biochim Biophys Acta 975:384–394

Reich PB, Walters MB, Ellsworth DS (1991) Leaf age and season influence the relationships between leaf nitrogen, leaf mass per area and photosynthesis in maple and oak trees. Plant Cell Environ 14:251–259

Reich PB, Walters MB, Ellsworth DS, Uhl C (1994) Photosynthesis-nitrogen relations in Amazonian tree species. Oecologia 97:62–72

Reich PB, Walters MB, Kloeppel BD, Ellsworth DS (1995) Different photosynthesis-nitrogen relations in deciduous hardwood and evergreen coniferous tree species. Oecologia 104:24–30

Reichstein M, Bahn M, Ciais P, Frank D, Mahecha MD, Seneviratne SI, Zscheischler J, Beer C, Buchmann N, Frank DC, Papale D, Rammig A, Smith P, Thonicke K, van der Velde K, Vicca S, Walz A, Wattenbach M (2013) Climate extremes and the carbon cycle. Nature 500:287–295

Richardson AD, Bailey AS, Denny EG, Martin CW, O'Keefe J (2006) Phenology of a northern hardwood forest canopy. Glob Change Biol 12:1174–1188

Richardson AD, Jenkins JP, Braswell BH, Hollinger DY, Ollinger SV, Smith ML (2007) Use of digital webcam images to track spring green-up in a deciduous broadleaf forest. Oecologia 152:323–334

Richardson AD, Black TA, Ciais P, Delbart N, Friedl MA, Gobron N, Hollinger DY, Kutsch WL, Longdoz B, Luyssaert S, Migliavacca M, Montagnani L, Munger JW, Moors E, Piao S, Rebmann C, Reichstein M, Saigusa N, Tomelleri E, Vargas R, Varlagin A (2010) Influence of spring and autumn phenological transitions on forest ecosystem productivity. Philos T R Soc B 365:3227–3246

Running S, Nemani R, Heinsch FA, Zhao M, Reeves M, Hashimoto H (2004) A continuous satellite-derived measure of global terrestrial primary production. Bioscience 54:547–560

Saigusa N, Yamamoto S, Murayama S, Kondo H (2005) Interannual variability of carbon budget components in an AsiaFlux forest site estimated by long-term flux measurements. Agr For Meteorol 134:4–16

Saigusa N, Yamamoto S, Hirata R, Ohtani Y, Ide R, Asanumae J, Gamoa M, Hirano T, Kondoa H, Kosugi Y, Li SG, Nakai Y, Takagi K, Tani M, Wanga H (2008) Temporal and spatial variations in the seasonal patterns of CO_2 flux in boreal, temperate, and tropical forests in East Asia. Agr For Meteorol 148:700–713

Saitoh TM, Nagai S, Saigusa N, Kobayashi H, Suzuki R, Nasahara KN, Muraoka H (2012) Assessing the use of camera-based indices for characterizing canopy phenology in relation to gross primary production in a deciduous broad-leaved and an evergreen coniferous forest in Japan. Ecol Inform 11:45–54

Sasai T, Ichii K, Yamaguchi Y, Nemani R (2005) Simulating terrestrial carbon fluxes using the new biosphere model "biosphere model integrating eco-physiological and mechanistic approaches using satellite data" (BEAMS). J Geophys Res 110(G2):G02014

Schaber J, Badeck FW (2003) Physiology-based phenology models for forest tree species in Germany. Int J Biometeorol 4:193–201

Sims DA, Gamon JA (2002) Relationships between leaf pigment content and spectral reflectance across a wide range of species, leaf structures and developmental stages. Remote Sens Environ 81:337–354

Tenhunen JD, Kabat P (1999) Integrating hydrology, ecosystem dynamics, and biogeochemistry in complex landscapes. Wiley, New York

Walther GR, Post E, Convey P, Menzel A, Parmesan C, Beebee TJC, Fromentin JM, Hoegh-Guldberg O, Bairlein F (2002) Ecological responses to recent climate change. Nature 416:389–395

Wang Q, Iio A, Tenhunen J, Kakubari Y (2008) Annual and seasonal variations in photosynthetic capacity of *Fagus crenata* along an elevation gradient in the Naeba Mountains, Japan. Tree Physiol 28:277–285

White M, Running S, Thornton P (1999) The impact of growing-season length variability on carbon assimilation and evapotranspiration over 88 years in the eastern US deciduous forest. Int J Biometeorol 42:139–145

Wilson KB, Baldocchi DD, Hanson PJ (2000) Spatial and seasonal variability of photosynthetic parameters and their relationship to leaf nitrogen in a deciduous forest. Tree Physiol 20:565–578

Wilson KB, Baldocchi DD, Hanson PJ (2001) Leaf age affects the seasonal pattern of photosynthetic capacity and net ecosystem exchange of carbon in a deciduous forest. Plant Cell Environ 24:571–583

Wright IJ, Reich PB, Westoby M, Ackerly DD, Baruch Z, Bongers F, Cavender-Bares J, Chapin T, Cornelissen JHC, Diemer M, Flexas J, Garnier E, Groom PK, Gulias J, Hikosaka K, Lamont BB, Lee T, Lee W, Lusk C, Midgley JJ, Navas ML, Niinemets Ü, Oleksyn J, Osada N, Poorter H, Poot P, Prior L, Pyankov VI, Roumet C, Thomas SC, Tjoelker MG, Veneklaas EJ, Villar R (2004) The worldwide leaf economics spectrum. Nature 428:821–827

Xu L, Baldocchi DD (2003) Seasonal trends in photosynthetic parameters and stomatal conductance of blue oak (*Quercus douglasii*) under prolonged summer drought and high temperature. Tree Physiol 23:865–877

Yamamoto S, Koizumi H (2005) Long-term carbon exchange at Takayama site, a cool-temperature deciduous forest in Japan. Agr For Meteorol 134:1–3

Yamamoto S, Murayama S, Saigusa N, Kondo H (1999) Seasonal and inter-annual variation of CO_2 flux between a temperate forest and the atmosphere in Japan. Tellus 51B:402–413

Yasumura Y, Ishida A (2011) Temporal variation in leaf nitrogen partitioning of a broad-leaved evergreen tree, *Quercus myrsinaefolia*. J Plant Res 124:115–123

Zhang X, Friedl MA, Schaaf CB, Strahler AH, Hodges JCF, Gao F, Reed BC, Huete A (2003) Monitoring vegetation phenology using MODIS. Remote Sens Environ 84:471–475